Malaria and leptospirosis co-infection: A mathematical model analysis with optimal control and cost-effectiveness analysis



Contents lists available at ScienceDirect

Scientific African

journal homepage: www.elsevier.com/locate/sciaf





Malaria and leptospirosis co-infection: A mathematical model analysis with optimal control and cost-effectiveness analysis

Habtamu Ayalew Engida*, Demeke Fisseha

Department of Applied Mathematics, Debre Markos University, Debre Markos, P.O. Box 269, Ethiopia

ARTICLE INFO

Editor name: B. Gyampoh

Keywords:
Malaria
Leptospirosis
Co-infection
Global stability
Optimal control
Numerical simulations
Cost-effective strategy

ABSTRACT

Malaria and leptospirosis are emerging vector-borne diseases that pose significant global health problems in tropical and subtropical regions. This study aimed to develop and analyze a mathematical model for the transmission dynamics of malaria-leptospirosis co-infection with optimal control measures. The model's dynamics are examined through its two sub-models: one for malaria alone and the other for leptospirosis alone. We apply a next-generation matrix approach to derive the basic reproduction numbers for the sub-models. By using the reproduction number, we demonstrate the local and global asymptotic stability of both diseasefree and endemic equilibria in these sub-models. We perform numerical experiments to validate the theoretical outcomes of the full co-infection model. The graphical results show that malarialeptospirosis co-infection will be eradicated from the population through time if R_{0ml} < 1. Conversely, if $R_{0ml} > 1$, the co-infection will persist in the population. Furthermore, we investigate an optimal control model to demonstrate the impact of various time-dependent controls in reducing the spread of both diseases and their co-infection. We use the forwardbackward sweep iterative method to perform numerical simulations of the optimal control problem. Our findings of the optimal control problem imply that strategy D, which incorporates all optimal controls, namely malaria prevention $\omega_1(t)$, leptospirosis prevention $\omega_2(t)$, insecticide control measure for malaria $\omega_3(t)$, control sanitation rate of the environment $\omega_4(t)$ is the most effective in minimizing our objective function. We also conduct a cost-effectiveness analysis to identify the predominant strategy in terms of cost among the optimal strategies.

Introduction

Malaria is an infectious disease of humans caused by protozoan parasites in the genus Plasmodium and transmitted by female Anopheles mosquitoes through their bites [1,2]. Human malaria is commonly caused by five species of Plasmodium parasites: P. falciparum, P. vivax, P. malariae, P. ovale wallikeri and P. ovale curtisi [3–5]. P.falciparum and P.vivax are the most prevalent and deadly malaria parasites, responsible for more than 95% of human infections worldwide [6]. P.falciparum is the most widespread and dangerous malaria parasite in African regions, particularly in the regions of sub-Saharan Africa. On the other hand, P.vivax is the predominant parasite outside of Africa, especially in the Americas and Asia [7]. Malaria infection continues to be a significant health problem, with a high number of cases and deaths reported in tropical and subtropical regions, particularly in Sub-Saharan Africa. According to the World Health Organization (WHO) report in 2021, there were approximately 247 million malaria cases and a total of 619 thousand deaths across 84 malaria-endemic countries worldwide. This is a significant rise compared to the 241 million cases reported in 2020 [8,9]. In 2021, 96% of global malaria deaths occurred in just 29 countries. Shockingly, four of

E-mail addresses: hayalew_engida@dmu.edu.et (H.A. Engida), demekefisseha@dmu.edu.et.com (D. Fisseha).

https://doi.org/10.1016/j.sciaf.2024.e02517

Received 20 April 2024; Received in revised form 17 December 2024; Accepted 24 December 2024

Available online 1 January 2025

2468-2276/© 2025 The Authors. Published by Elsevier B.V. This is an open access article under the CC BY-NC-ND license (http://creativecommons.org/licenses/by-nc-nd/4.0/).

^{*} Corresponding author.

these countries (Nigeria, the Democratic Republic of the Congo, Tanzania, and Niger) accounted for 52% of all malaria deaths globally. Of the estimated malaria cases reported in 2021, 234 million cases (95%) occurred in the WHO African region [10]. The WHO recently reported an estimated 249 million malaria cases and 608,000 deaths in 85 malaria-endemic countries in 2022. This marked a significant increase in cases compared to 2021. The main country contributor to the increase was Pakistan, followed by Ethiopia, Nigeria, and Uganda, according to WHO. Of the estimated cases reported in 2022, 94% (233 million cases) were in the WHO African region, with Nigeria (27%), the Democratic Republic of the Congo (12%), Uganda (5%) and Mozambique (4%), which together accounted for about 50% of global malaria cases. Moreover, about 96% of malaria deaths globally were in 29 countries, with Nigeria (31%), the Democratic Republic of the Congo (12%), Niger (6%) and the United Republic of Tanzania (4%) responsible for more than half of all malaria deaths worldwide in 2022 [1,11].

Leptospirosis is a zoonotic bacterial disease caused by pathogenic species in the genus Leptospira. It affects both humans and animals [12–14]. Rodents, such as rats and mice, are the main carriers of Leptospira globally, especially in tropical and sub-tropical regions like Southeast Asia and Sub-Sahara Africa, where the disease is endemic [15,16]. The pathogen is mainly found in the urine of infected animals (rodents) and can survive in moist soil and water [17,18]. The rodent-born leptospirosis is transmitted to humans or other rodents most commonly through contact with soil or water that has been contaminated by the urine of infected rodents, or through contact with the urine of leptospirosis-infected rodents [19–21]. Leptospirosis transmission from person to person is very rare [22]. According to recent reports, the incidence of leptospirosis was estimated to be 1.03 million cases worldwide, of which 58.9 thousand ended with death [23,24].

Co-infection involves the simultaneous infection of a single host by various pathogen species. It also occurs when two or more pathogen variants (genetic variations of the same pathogen) infect a single host simultaneously [25,26]. Nowadays, co-infection of infectious diseases is a major medical concern, significantly contributing to increased mortality rates globally. Approximately 30% of human infections are likely co-infections, with this rate potentially reaching 80% in some human communities [27]. Malaria and leptospirosis are bacterial diseases that cause global health problems with overlapping geographic distribution, especially in tropical and subtropical areas, suggesting a high potential for the coexistence of Plasmodium and Leptospira in the same individual. Indeed, several studies have well-documented malaria-leptospirosis co-infection cases in the human population. [28] quantified the prevalence of malaria and leptospirosis co-infection among febrile patients in various tropical and subtropical countries. They also investigated the association between the two infections. Likewise, [29] reported a high number of malaria-leptospirosis co-infections in their study. The study suggests that managing malaria and leptospirosis co-infection is challenging due to their similar clinical presentations and the readily available confirmatory diagnosis for malaria compared to leptospirosis. Focusing treatment on malaria mono-infections may delay specific therapy for leptospirosis and vice versa. According to the findings in [30], 23.4% of leptospirosis patients have malaria cases. Moreover, in [31–33], the authors described malaria-leptospirosis co-infection cases in areas where both diseases are endemic.

Mathematical modeling has become a vital discipline in studying the dynamics of infectious diseases using mathematical tools. It helps in gaining a better understanding of disease transmission dynamics, predicting the outcome of disease spread, and suggesting appropriate health control measures for disease eradication in the population. In particular, mathematical models with optimal control theory play an essential role in devising cost-effective strategies to quantify and mitigate disease spread [34–36].

A lot of mathematical models have been developed to study the dynamics of malaria transmission from various perspectives. [37] presented a mathematical model to assess the impact of relapse and reinfection on the transmission dynamics of malaria. Their findings highlighted that both reinfection and relapse significantly influence malaria dynamics. [38] proposed a mathematical model to analyze the effect of seasonality and ivermectin on malaria transmission, while [39] investigated a deterministic model to show the effect of drug-resistance strains, treatment, and use of misquotes nets on the transmission dynamics of malaria in Nigeria. [40] developed a mathematical model using impulsive partial differential equations to assess the effectiveness of indoor residual spraying (IRS) in reducing malaria transmission. Furthermore, several scholars have applied the optimal control theory to eradicate malaria infection by incorporating various factors in malaria models. In [41], Dipo Aldila and Michellyn Angelina developed a mathematical model for malaria transmission dynamics, focusing on the implications of vector bias and the application of optimal control strategies. Another study [42] examined a mathematical model for malaria transmission dynamics with and without seasonal factors in mosquito populations and also incorporated optimal control measures like insecticides, prevention, and treatment. Authors in [43] formulated a two-group mathematical model by age distinguishing between vaccinated and unvaccinated populations for malaria transmission that incorporates vaccination strategies. The authors used optimal control theory to assess strategies that minimize malaria infections. The findings highlighted the importance of combining vaccination with other interventions, such as treatment and personal protection to achieve optimal outcomes. Likewise, many other researchers have applied optimal control theory to assess intervention strategies for malaria, incorporating factors such as vector bias, relapse, reinfection, and vaccination into mathematical models to better understand and reduce malaria transmission (see [44-46]).

Some other researchers have developed the co-infection of malaria with other infectious diseases such as HIV [47], cholera [48], leishmaniasis [49], and COVID-19 [50–52]. On the other hand, [53] studied a compartmental model for leptospirosis and dengue co-infection in the absence of optimal controls that incorporates susceptible, infected, and recovered individuals for both diseases.

The dynamics of leptospirosis transmission in the absence of optimal controls have been described by several mathematical models. [54] developed a deterministic mathematical model for the transmission dynamics of leptospirosis. [55] proposed a mathematical model for the dynamic behavior of leptospirosis with saturated incidence. They examined the stability analysis of the steady states of their model. [56] modeled the dynamics of leptospirosis using a compartmental approach. Also, [57] developed and examined a mathematical model for the dynamics of leptospirosis transmission in human, rodent and bacterial populations. While, mathematical studies [58–61] have explored the dynamics of leptospirosis using the application of the optimal control theory. The

primary aim of infectious disease modeling is to develop effective interventions for controlling and ultimately eradicating diseases. Additionally, mathematical models that employ the optimal control theory are essential for developing cost-effective interventions to achieve these objectives. Leptospirosis-malaria co-infection is common in tropical and subtropical regions due to their similar geographical distributions. Both diseases share similarities in clinical symptoms. The prevalence of their co-infection cases has been reported subsequently in the literature. To the best of our knowledge, the dynamics of malaria and leptospirosis co-infection transmission has not been described by a compartmental mathematical model. This overlooked aspect motivates us to study the co-infection dynamics between malaria and leptospirosis. The goal of this study is to propose a novel deterministic mathematical model that provides a detailed analysis of the qualitative and quantitative dynamics of malaria-leptospirosis co-infection. Thus, we develop and rigorously analyze a mathematical model for malaria-leptospirosis co-infection, which incorporates their key biological and epidemiological characteristics. We shall also explore an optimal control model of malaria-leptospirosis co-infection by integrating four control measures: two for malaria (prevention against mosquito bites and insecticide control measures) and another two controls for leptospirosis (leptospirosis prevention and the control sanitation rate of the environment). We apply optimal control theory to identify the most effective strategies (in terms of efficacy and cost). The study employs Pontryagin's maximum principle (PMP) to solve the optimal control model.

The paper is structured as follows: In Section "Model formulation", we present the formulation of our proposed co-infection model. In Section "Model analysis", we present the detailed analytical analysis of this model, with Section "Malaria-only model" and Section "Leptospirosis-only model" focusing on the malaria-only and leptospirosis-only sub-models, respectively, and Section "Malaria-leptospirosis model" presents the full malaria-leptospirosis co-infection model. The numerical simulations of the autonomous model and discussions are given in Section "Numerical simulations". Also, the optimal control model and its mathematical analysis are presented in Section "Optimal control analysis of the malaria-leptospirosis model". Finally, we conclude the paper in Section "Conclusion".

Model formulation

To formulate the transmission dynamics of the malaria-leptospirosis co-infection model, we consider three population groups at time t: a human population $N_h(t)$, a mosquito population $N_q(t)$ and a rodent population $N_r(t)$. At any time t the total human population is grouped into nine epidemiological states: susceptible humans $S_h(t)$, humans exposed to malaria $E_m(t)$, humans infected with malaria $I_m(t)$, humans exposed to leptospirosis $E_l(t)$, humans infected with leptospirosis $I_l(t)$, humans infected with both malaria and leptospirosis $I_m(t)$, humans recovered from malaria $R_m(t)$, humans recovered from leptospirosis $R_l(t)$, humans recovered from both malaria and leptospirosis $R_m(t)$. Thus,

$$N_h(t) = S_h(t) + E_m(t) + I_m(t) + I_l(t) + I_l(t) + I_m(t) + R_m(t) + R_l(t) + R_m(t).$$

$$\tag{1}$$

While the total mosquito and rodent populations are subdivided into the following states: $S_q(t)$ and $I_q(t)$ representing susceptible mosquitoes and infected mosquitoes, respectively; $S_r(t)$ and $I_r(t)$ representing susceptible rodents and infected rodents, respectively. The total mosquito population $N_q(t)$ and the total rodent population $N_r(t)$ are given by

$$N_a(t) = S_a(t) + I_a(t), \quad N_r(t) = S_r(t) + I_r(t).$$
 (2)

Also, the concentration of the pathogens in the environment at time t is represented by B(t). The recruitment rates for human, malaria and rodent populations, are denoted by Λ , Λ_q and Λ_r , respectively. Susceptible humans could become infected with malaria, at a rate of $\lambda_m = \frac{\beta_{hm}\hat{\beta}_0 I_q}{N_h}$, where β_{hm} is the probability of malaria transmission per bite in humans and β_0 is the biting rate of mosquitoes per day. Susceptible humans could also acquire leptospirosis, at a rate of $\lambda_l = \frac{\beta_{he}B}{\kappa + B} + \beta_{hr}I_r$, where β_{he} and β_{hr} are leptospirosis transmission rates in humans, the nonlinear term $\frac{B}{\kappa+B}$ is contact probability between susceptible humans and contaminated environment, and the constant κ is the pathogen concentration. Infectious individuals with malaria could become infected with leptospirosis at a rate of $\tau_1 \lambda_l$, while infectious individuals with leptospirosis could become infected with malaria at a rate $\tau_2 \lambda_m$, where the coefficients τ_1 and τ_2 represent susceptibility to a second infection. It makes sense that those who have one of the diseases will be more susceptible to getting the other since both malaria and leptospirosis affect the immune system. τ_1 and τ_2 δ (satisfying $\tau_1, \tau_2 \ge 1$) are the modification parameters that account for the increased infectiousness of co-infected persons caused by each disease. Susceptible mosquitoes could acquire malaria infection, at a rate of $\lambda_q = \frac{\beta_q \beta_0 (I_m + I_{ml})}{N_h}$, where β_q is the probability of malaria transmission in mosquitoes. While, susceptible rodents could acquire leptospirosis infection, at a rate of $\lambda_r = \frac{\beta_r B}{\kappa + B}$, where β_r is leptospirosis transmission rate in rodents. Moreover, the recovery rate from the co-infected class is represented by θ , individuals in this class may transfer to either malaria only infectious at a leptospirosis recovery rate of $\xi_1\theta$, transfer to leptospirosis only infectious at a malaria recovery rate of $\xi_2\theta$, or become recovered from both diseases at a rate of $(1-(\xi_1+\xi_2))\theta$, where ξ_1 and ξ_2 fractions between 0 and 1. Furthermore, individuals in I_m recover a rate of γ_m , and they become susceptible humans or recovered humans with probabilities of ζ and $1-\zeta$, respectively, where $\zeta \in (0,1)$. It is assumed that there is a higher chance of individuals in I_m becoming susceptible than individuals recovered from this class (i.e, $\zeta > (1 - \zeta)$). In the formulation of the model, additional assumptions are made as follows:

- (i) Humans could acquire malaria infection through contact with infected mosquitoes, while susceptible mosquitoes could acquire malaria infection through contact with malaria-infected humans or co-infected humans [37,50].
- (ii) Humans acquire infection of leptospirosis through either contact with infected rodents or contact with contaminated environments (soil or water) [20,21,57].

Table 1
Description of parameters of the model (3).

| Parameter | Description | Value | Source |
|--------------------------|------------------------------------------------------------------|----------------------------------------------------|---------|
| Λ | Human population recruitment rate | $\mu \times N_h(0)$ Humans day ⁻¹ | [61] |
| β_{hm} | Probability of malaria transmission in humans per bite | 0.0044 Day ⁻¹ | [39,62] |
| α_m | Progression rate from exposed class to malaria infectious humans | 0.0833 Day ⁻¹ | [43] |
| γ_m | Recovery rate of malaria infectious humans | 0.00014 Day ⁻¹ | [42,63] |
| ρ_m | Waning immunity rate of $R_m(t)$ | 0.005 Day ⁻¹ | [42,63] |
| μ | Natural death rate of humans | $\frac{1}{70 \times 365}$ Day ⁻¹ | [39,42] |
| β_0 | Mosquitoes biting rate | 1 | [37,47] |
| β_{he} | leptospirosis transmission rate in humans from the environment | 0.00047 | Assumed |
| β_{hr} | leptospirosis transmission rate in humans from rodents | 0.0004 | Assumed |
| α_l | Progression rate from exposed to leptospirosis-infected humans | 0.003 Day ⁻¹ | [60] |
| γ_l | Recovery rate of leptospirosis infected humans | 0.0027 Day ⁻¹ | [53] |
| ρ_l | Waning immunity rate of $R_l(t)$ | 0.00285 Day ⁻¹ | [53,60] |
| θ | Recovery rate of co-infection | 0.00014 Day ⁻¹ | Assume |
| τ_1 | Modification parameter for enhancing leptospirosis infection | 1.02 | [37,39] |
| | in humans due to malaria infection | | |
| τ_2 | Modification parameter for enhancing malaria infection | 1.01 | [37,39] |
| | in humans due to malaria infection | | |
| ξ_1 | Recovery rate of leptospirosis in co-infected class | 0.45 | Assume |
| ξ_2 | Recovery rate of malaria in co-infected class | 0.35 | Assume |
| ζ | Probability of individual in I_m becoming susceptible human | 0.75 | Assume |
| Λ_q | Recruitment rate of mosquitoes | $\mu_q \times N_q(0)$ mosquitoes day ⁻¹ | Assume |
| β_q | Malaria transmission rate in mosquitoes | 0.0044 | [39,64] |
| μ_q | Natural mortality rate of Mosquitoes | $\frac{1}{15}$ Day ⁻¹ | [64,65] |
| Λ_r | Recruitment rate of rodents | 0.285 rodents day ⁻¹ | [59] |
| β_r | Leptospirosis transmission rate in rodents | 0.000003 | [59] |
| μ_r | Natural mortality rate of rodents | 0.0018 Day ⁻¹ | [58] |
| μ_b | Bacteria removal rate | 0.05 Day ⁻¹ | [57,61] |
| κ | Pathogenic concentration in environment | 7000 pathogens | Assume |
| ϵ_1, ϵ_2 | shading rates of B from I_l and I_{ml} , respectively | $\log_{10}(8.1 \times 10^8)$ day ⁻¹ | Assume |
| ϵ_3 | The rates at which the size of B increase by class I_r | $\log_{10}(8.1 \times 10^8) \text{ day}^{-1}$ | [59] |

- (iii) Rodents acquire infection of leptospirosis through contact with contaminated environments (soil or water).
- (iv) We assumed that humans with malaria are susceptible to infection with leptospirosis and vice versa based on several case reports on the co-infection of the two diseases [28,30,33].
- (v) Also assumed homogeneous mixing between human and rodent populations [57].
- (vi) The incidence from the contaminated environment to humans is assumed to be modeled logistically [57,61].

The description, values and sources of the model parameters are given in Table 1 whereas flow diagram of the model is provided in Fig. 1.

From Fig. 1, the model is described by the following system of non-linear ODEs.

$$\begin{array}{ll} \frac{dS_{h}}{dl} &= \Lambda + \zeta \gamma_{m} I_{m} + \rho_{m} R_{m} + \rho_{l} R_{l} + \rho_{ml} R_{ml} - \left(\lambda_{m} + \lambda_{l} + \mu\right) S_{h}, & \frac{dR_{l}}{dk_{ml}} &= \gamma_{l} I_{l} - (\rho_{l} + \mu) R_{l}, \\ \frac{dE_{m}}{dt} &= \lambda_{m} S_{h} - (\alpha_{m} + \mu) E_{m}, & \frac{dS_{l}}{dk_{ml}} &= (1 - (\xi_{1} + \xi_{2}))\theta I_{ml} - (\rho_{ml} + \mu) R_{ml}, \\ \frac{dS_{l}}{dt} &= \alpha_{m} E_{m} + \xi_{1} \theta I_{ml} - (\gamma_{m} + \mu + \tau_{1} \lambda_{l}) I_{m}, & \frac{dS_{l}}{dt} &= \Lambda_{q} - \left(\lambda_{q} + \mu_{q}\right) S_{q}, \\ \frac{dE_{l}}{dt} &= \lambda_{l} S_{h} - (\alpha_{l} + \mu) E_{l}, & \frac{dI_{q}}{dt} &= \lambda_{q} S_{q} - \mu_{q} I_{q}, \\ \frac{dI_{l}}{dt} &= \alpha_{l} E_{l} + \xi_{2} \theta I_{ml} - (\gamma_{l} + \mu + \tau_{2} \lambda_{m}) I_{l}, & \frac{dS_{r}}{dt} &= \Lambda_{r} - \left(\lambda_{r} + \mu_{r}\right) S_{r}, \\ \frac{dI_{ml}}{dt} &= \tau_{1} \lambda_{l} I_{m} + \tau_{2} \lambda_{m} I_{l} - (\theta + \mu) I_{ml}, & \frac{dI_{r}}{dt} &= \lambda_{r} S_{r} - \mu_{r} I_{r}, \\ \frac{dR_{m}}{dt} &= (1 - \zeta) \gamma_{m} I_{m} - (\rho_{m} + \mu) R_{m}, & \frac{dB}{dt} &= \epsilon_{1} I_{l} + \epsilon_{2} I_{ml} + \epsilon_{3} I_{r} - \mu_{b} B, \end{array} \tag{3}$$

where,
$$\lambda_m = \frac{\beta_{hm}\beta_0I_q}{N_h}$$
, $\lambda_l = \frac{\beta_{he}B}{\kappa+B} + \beta_{hr}I_r$, $\lambda_q = \frac{\beta_q\beta_0(I_m+I_{ml})}{N_h}$, $\lambda_r = \frac{\beta_rB}{\kappa+B}$.

Model analysis

In this section, we consider the qualitative analysis of the two sub-models of the model system (3), as well as the full co-infection model.

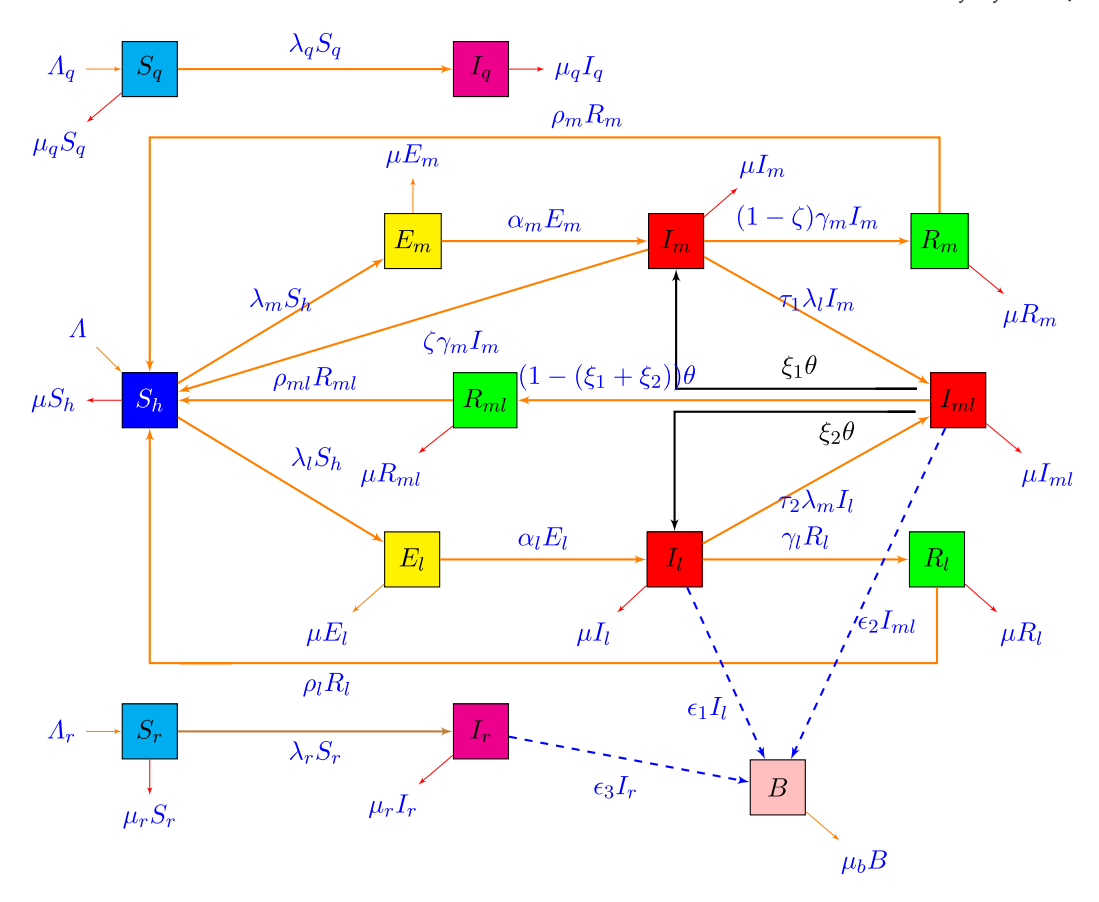


Fig. 1. The flow diagram of the model.

Malaria-only model

By setting $E_l(t) = I_l(t) = I_{ml}(t) = R_{ll}(t) = R_{ml}(t) = S_r(t) = I_r(t) = B_l(t) = 0$ in (3), we obtained the following malaria only model:

setting
$$E_l(t) = I_l(t) = I_{ml}(t) = R_l(t) = R_{ml}(t) = S_r(t) = I_r(t) = B_l(t) = 0$$
 in (3), we obtained the following malaria only model:
$$\begin{cases} \frac{dS_h}{dt} = \Lambda + \zeta \gamma_m I_m + \rho_m R_m - \left(\frac{\beta_{hm}\beta_0 I_q}{N_h} + \mu\right) S_h, \\ \frac{dE_m}{dt} = \frac{\beta_{hm}\beta_0 I_q}{N_h} S_h - (\alpha_m + \mu) E_m, \\ \frac{dI_m}{dt} = \alpha_m E_m - (\gamma_m + \mu) I_m, \\ \frac{dR_m}{dt} = (1 - \zeta) \gamma_m I_m - (\rho_m + \mu) R_m, \\ \frac{dS_q}{dt} = \Lambda_q - \left(\frac{\beta_q \beta_0 I_m}{N_h} + \mu_q\right) S_q, \\ \frac{dI_q}{dt} = \frac{\beta_q \beta_0 I_m}{N_h} S_q - \mu_q I_q, \end{cases}$$

$$(4)$$

where

$$N_h = S_h + E_m + I_m + R_m. ag{5}$$

Consider the region

$$\Pi_{m} = \left\{ (S_{h}, E_{m}, I_{m}, R_{m}, S_{q}, I_{q}) \in R_{+}^{6} : N_{h} \leq \frac{\Lambda}{\mu}, N_{q} \leq \frac{\Lambda_{q}}{\mu_{q}} \right\}.$$
(6)

It is easy to show (see, for example, [47,50]) that all solutions of the system (4) starting in Π_m will remain in this region for all $t \ge 0$. As a result, Π_m is positively invariant and attracts all solutions of (4) [66]. Thus, it is sufficient to study the dynamics of the model (4) in Π_m .

Stability of the disease free equilibrium of the malaria-only model

The disease-free equilibrium (DFE) of the malaria-only model system (4) is obtained by setting each of the equations of the system (4) to zero and solving for S_h and S_q . Also, at the DFE there are no infections and recovery. Thus, the DFE point of the system (4) is given by

$$\epsilon_{0m}^* = \left(S_h^*, 0, 0, 0, S_q^*, 0\right) = \left(\frac{\Lambda}{\mu}, 0, 0, 0, \frac{\Lambda_q}{\mu_q}, 0\right). \tag{7}$$

By applying the method of the next-generation matrix [67] to the system (4), the associated basic reproduction number (R_{0m}) is obtained as follows: The new infection terms F(t) and the rate of transfer of individuals to the compartments V(t) are given by:

$$F(t) = \begin{pmatrix} \frac{\beta_{hm}\beta_0 I_q}{N_h} S_h \\ 0 \\ \frac{\beta_q \beta_0 I_m}{N_h} S_q \end{pmatrix}, \text{ and } V(t) = \begin{pmatrix} (\alpha_m + \mu)E_m \\ -\alpha_m E_m + (\gamma_m + \mu)I_m \\ \mu_q I_q \end{pmatrix}.$$

Thus, the associated Jacobian matrices of F(t) and V(t) at e_{0m}^* are denoted by F and V, respectively, given as follows:

$$F = \begin{pmatrix} 0 & 0 & \beta_{hm}\beta_0 \\ 0 & 0 & 0 \\ 0 & \frac{\beta_q\beta_0\Lambda_q\mu}{\Lambda\mu_q} & 0 \end{pmatrix}, \text{ and } V = \begin{pmatrix} (\alpha_m + \mu) & 0 & 0 \\ -\alpha_m & (\gamma_m + \mu) & 0 \\ 0 & 0 & \mu_q \end{pmatrix}$$

Therefore, the basic reproduction number of the malaria only model (4) is given by

$$R_{0m} = \rho(FV^{-1}) = \sqrt{\frac{\Lambda_q \beta_{hm} \beta_q \beta_0^2 \mu \alpha_m}{\Lambda \mu_q^2 (\alpha_m + \mu)(\gamma_m + \mu)}}.$$
(8)

Thus, based on Theorem 2 of [67], the following result is established.

Theorem 1. The DFE, e_{0m}^* , of malaria-only model system (4) is locally asymptotically stable if $R_{0m} < 1$ and unstable if $R_{0m} > 1$.

Global asymptotic stability of DFE of the malaria-only model

We follow the direct Lyapunov method [68], to establish the global asymptotic stability of ϵ_{0m}^* , which requires a scalar function $\Gamma_0(\chi), \chi \in \mathbb{R}^6$ defined on an open set, U_0 in Π_m , containing ϵ_{0m}^* and satisfying the following conditions.

- (i) $\Gamma_0(\epsilon_{0m}^*) = 0$,
- (ii) $\Gamma_0(\chi) > 0$, for all $\chi \in U_0 \setminus \epsilon_{0m}^*$, (iii) $\frac{d\Gamma_0}{dt} < 0$, for all $\chi \in U_0 \setminus \epsilon_{0m}^*$ and $\frac{d\Gamma_0}{dt} = 0$ at ϵ_{0m}^* .

The following result is established for global asymptotic stability of $\epsilon_{0...}^*$.

Theorem 2. The DFE, ϵ_{0m}^* , given by (7) of the malaria-only model system (4) is globally asymptotically stable (GAS) if $R_{0m} \leq 1$.

Proof. If $R_{0m} < 1$, there is a unique locally asymptotically stable DFE accordingly Theorem 1. Consider the following a Lyapunov

$$\Gamma_0(E_m,I_m,I_q) = \mu_m E_m + \frac{\mu_q(\alpha_m + \mu)}{\alpha_m} I_m + \beta_{hm} \beta_0 I_q. \label{eq:gamma_def}$$

The time derivative of Γ_0 derived along the solutions of the model system (4) is given by

$$\Gamma_{0}' = \mu_{q} E_{m}' + \frac{\mu_{q}(\alpha_{m} + \mu)}{\alpha_{m}} I_{m}' + \beta_{hm} \beta_{0} I_{q}'$$

$$= \mu_{q} \left(\frac{\beta_{hm} \beta_{0} I_{q}}{N_{h}} S_{h} - (\alpha_{m} + \mu) E_{m} \right) + \frac{\mu_{q}(\alpha_{m} + \mu)}{\alpha_{m}} \left(\alpha_{m} E_{m} - (\gamma_{m} + \mu) I_{m} \right) + \beta_{hm} \beta_{0} \left(\frac{\beta_{q} \beta_{0} I_{m}}{N_{h}} S_{q} - \mu_{q} I_{q} \right).$$
(9)

Note that
$$\frac{S_h}{N_h} < 1$$
 and $S_m \leq \frac{\Lambda_q}{\mu_q}$ in $U_0 \setminus \epsilon_{0m}^*$. It follows from (9) that
$$\Gamma_0' < \mu_q \Big(\beta_{hm}\beta_0I_q - (\alpha_m + \mu)E_m\Big) + \frac{\mu_q(\alpha_m + \mu)}{\alpha_m} \Big(\alpha_m E_m - (\gamma_m + \mu)I_m\Big) + \beta_{hm}\beta_0 \Big(\frac{\beta_q\beta_0\Lambda_q\mu I_m}{\Lambda\mu_q} - \mu_qI_q\Big)$$

$$< \beta_{hm}\beta_0\mu_qI_q - \mu_q(\alpha_m + \mu)E_m + \mu_q(\alpha_m + \mu)E_m - \frac{\mu_q(\alpha_m + \mu)}{\alpha_m} (\gamma_m + \mu)I_m + \frac{\beta_q\beta_{hm}\beta_0^2\Lambda_q\mu I_m}{\Lambda\mu_q} - \beta_{hm}\beta_0\mu_qI_q\Big)$$

$$< \Big(\frac{\beta_q\beta_{hm}\beta_0^2\Lambda_q\mu}{\Lambda\mu_q} - \frac{\mu_q(\alpha_m + \mu)(\gamma_m + \mu)}{\alpha_m}\Big)I_m$$

$$< \frac{\mu_q(\alpha_m + \mu)(\gamma_m + \mu)}{\alpha} \Big(R_{0m}^2 - 1\Big)I_m \leq 0 \text{ when } R_{0m} \leq 1.$$

Since the model parameters are non-negative, $\Gamma_0'(t) < 0$ in $U_0 \setminus \epsilon_{0m}^*$ and if $R_{0m} \le 1$, and $\Gamma_0' = 0$ if and only if $E_m = I_m = I_q = 0$ (or at ϵ_{0m}^*). Thus, based on Lasalle's Invariance Principle [68], $\left(E_m(t), I_m(t), I_q(t)\right) \to (0, 0, 0)$ as $t \to \infty$. Substituting the relation $\left(E_m(t), I_m(t), I_q(t)\right) = (0, 0, 0)$ into the model system (4) yields the following system

$$\begin{pmatrix} S_h'(t) \\ R_m'(t) \\ S_g'(t) \end{pmatrix} = \begin{pmatrix} \Lambda + \rho_m R_m - \mu S_h \\ -(\rho_m + \mu) R_m \\ \Lambda_q - \mu_q S_q \end{pmatrix}.$$
(10)

The solutions for 2nd and the 3rd linear ODEs of (10) can be easily found as:

$$R_m(t) = R_m(0)e^{-(\rho_m + \mu)t}, \quad S_q(t) = \frac{\Lambda_q}{\mu_q} \left(1 - e^{-\mu_q t} \right) + S_q(0)e^{-\mu_q t}. \tag{11}$$

It follows from (11) that $R_m(t) \to 0$ and $S_q(t) \to \frac{\Lambda_q}{\mu_q}$ as $t \to \infty$, regardless of the initial population sizes $R_m(0)$ and $S_q(0)$. Lastly, using the first equation of (10) and (11), we get

$$S'_{L}(t) = \Lambda + \rho_{m} R_{m}(0) e^{-(\rho_{m} + \mu)t} - \mu S_{L}(t).$$
 (12)

Solving (12), yields

$$S_h(t) = \frac{\Lambda}{\mu} + S_h(0)e^{-\mu t} - R_m(0)e^{-(\rho_m + \mu)t}.$$
(13)

Clearly, $S_h(t) \to \frac{\Lambda}{\mu}$, as $t \to \infty$, with the initial population size. Consequently, every solution trajectory of the system (4) with the initial population size in Π_m converges to ϵ_{0m}^* as $t \to \infty$ when $R_{0m} \le 1$. Biologically, this indicates that the susceptible individuals do not get additional infections if $R_{0m} \le 1$. Thus, the malaria infection can be eliminated from the population in the long term if $R_{0m} \le 1$.

Existence of the endemic equilibrium of the malaria-only model

The endemic equilibrium point of the model (4) is a state, which is the solution set to the following system.

$$\begin{cases} \Lambda + \zeta \gamma_m I_m^* + \rho_m R_m^* - \left(\lambda_m^* + \mu\right) S_h^* = 0, \\ \lambda_m^* S_h^* - (\alpha_m + \mu) E_m^* = 0, \\ \alpha_m E_m^* - (\gamma_m + \mu) I_m^* = 0, \\ (1 - \zeta) \gamma_m I_m^* - (\rho_m + \mu) R_m^* = 0, \\ \Lambda_q - \left(\frac{\beta_q \beta_0 I_m^*}{N_h^*} + \mu_q\right) S_q^* = 0, \\ \frac{\beta_q \beta_0 I_m^*}{N_h^*} S_q^* - \mu_q I_q^* = 0, \end{cases}$$

$$(14)$$

where,

$$\lambda_m^* = \frac{\beta_{hm}\beta_0 I_q^*}{N^*} \tag{15}$$

Solving the system of Eqs. (14) at the endemic equilibrium denoted by $\epsilon_{1m}^* = \left(S_h^*, E_m^*, I_m^*, R_m^*, S_q^*, I_q^*\right)$, yields, $S_h^* = \frac{\Lambda_+ \zeta \gamma_m I_m^* + \rho_m R_m^*}{(\lambda_m^* + \mu)}$, $E_m^* = \frac{\phi_2}{\alpha_m} I_m^*, R_m^* = \frac{(1 - \zeta)\gamma}{\phi_3} I_m^*, S_q^* = \frac{\Lambda_q N_h^*}{\beta_q \beta_0 I_m^* + \mu_q N_h^*}$,

$$I_{m}^{*} = \frac{\Lambda \alpha_{m} \phi_{3} \lambda_{m}^{*}}{\phi_{1} \phi_{2} \phi_{3} \mu + \lambda_{m}^{*} \left[\alpha_{m} \gamma_{m} \mu (1 - \zeta) + \phi_{3} \left(\alpha_{m} \mu + \mu \phi_{2} \right) \right]}, I_{q}^{*} = \frac{\Lambda_{q} \beta_{q} \beta_{0} I_{m}^{*}}{\mu_{q}^{2} N_{h}^{*} + \beta_{q} \beta_{0} \mu_{q} I_{m}^{*}},$$

$$(16)$$

where, $\phi_1 = \alpha_m + \mu$, $\phi_2 = \gamma_m + \mu$, and $\phi_3 = \rho_m + \mu$.

The Eq. (15), yields

$$I_q^* = \frac{\lambda_m^* N_h^*}{\beta_{hm} \beta_0}. (17)$$

Note that N_h^* denotes the value of N_h at ϵ_{1m}^* , solving for it at ϵ_{1m}^* , gives $N_h = \frac{\Lambda}{\mu}$. Thus, by combining the Eqs. (16) and (17), we obtain the following quadratic polynomial equation in λ_m^* given by

$$\lambda_m^*(A_1\lambda_m^* + A_0) = 0, (18)$$

where

$$A_1 = \frac{\varLambda^2}{\mu^2} \mu_q^2 \left[\alpha_m \gamma_m \mu (1-\zeta) + \phi_3 \left(\alpha_m (\delta_m + \mu) + \mu \phi_2 \right) \right] + \frac{\varLambda^2}{\mu} \beta_q \beta_0 \alpha_m \mu_q \phi_3, \quad \text{and} \quad \lambda_q = \frac{\Lambda^2}{\mu^2} \mu_q^2 \left[\alpha_m \gamma_m \mu (1-\zeta) + \phi_3 \left(\alpha_m (\delta_m + \mu) + \mu \phi_2 \right) \right] + \frac{\Lambda^2}{\mu^2} \beta_q \beta_0 \alpha_m \mu_q \phi_3, \quad \lambda_q = \frac{\Lambda^2}{\mu^2} \mu_q^2 \left[\alpha_m \gamma_m \mu (1-\zeta) + \phi_3 \left(\alpha_m (\delta_m + \mu) + \mu \phi_2 \right) \right] + \frac{\Lambda^2}{\mu^2} \beta_q \beta_0 \alpha_m \mu_q \phi_3, \quad \lambda_q = \frac{\Lambda^2}{\mu^2} \mu_q^2 \left[\alpha_m \gamma_m \mu (1-\zeta) + \phi_3 \left(\alpha_m (\delta_m + \mu) + \mu \phi_2 \right) \right] + \frac{\Lambda^2}{\mu^2} \beta_q \beta_0 \alpha_m \mu_q \phi_3, \quad \lambda_q = \frac{\Lambda^2}{\mu^2} \mu_q^2 \left[\alpha_m \gamma_m \mu (1-\zeta) + \phi_3 \left(\alpha_m (\delta_m + \mu) + \mu \phi_2 \right) \right] + \frac{\Lambda^2}{\mu^2} \beta_q \beta_0 \alpha_m \mu_q \phi_3, \quad \lambda_q = \frac{\Lambda^2}{\mu^2} \mu_q^2 \left[\alpha_m \gamma_m \mu (1-\zeta) + \phi_3 \left(\alpha_m (\delta_m + \mu) + \mu \phi_2 \right) \right] + \frac{\Lambda^2}{\mu^2} \beta_q \beta_0 \alpha_m \mu_q \phi_3, \quad \lambda_q = \frac{\Lambda^2}{\mu^2} \mu^2 \left[\alpha_m \gamma_m \mu (1-\zeta) + \phi_3 \left(\alpha_m (\delta_m + \mu) + \mu \phi_2 \right) \right] + \frac{\Lambda^2}{\mu^2} \beta_q \beta_0 \alpha_m \mu_q \phi_3, \quad \lambda_q = \frac{\Lambda^2}{\mu^2} \mu^2 \left[\alpha_m \gamma_m \mu (1-\zeta) + \phi_3 \left(\alpha_m (\delta_m + \mu) + \mu \phi_2 \right) \right]$$

$$A_0 = \frac{\Lambda^2}{\mu} \mu_q^2 \phi_1 \phi_2 \phi_3 \left(1 - R_{0m}^2 \right).$$

Clearly, the coefficient A_1 is always positive and A_0 is positive if and only if $R_{0m} < 1$. Thus, the quadratic Eq. (18) has a unique positive solution given by $\lambda_m^* = -\frac{A_0}{A_1}$ when $R_{0m} > 1$, which is feasible (or biologically meaningful). This indicates that the model system (4) has a unique positive endemic equilibrium if $R_{0m} > 1$. On the other hand, $A_0 \ge 0$ for $R_{0m} \le 1$, as a result $\lambda_m^* = -\frac{A_0}{A_1} \le 0$, which is not feasible biologically. As a result, the model system (4) has no positive endemic equilibrium when $R_{0m} \le 1$. Furthermore, the result shows that the system (4) has no chance of experiencing backward bifurcation. Consequently, we have established the following result.

Theorem 3 (Existence of the Endemic Equilibrium). The malaria-only model (4) has

- (i) a unique positive endemic equilibrium if $R_{0m} > 1$,
- (ii) no endemic equilibrium otherwise.

Global asymptotic stability of the endemic equilibrium of the malaria-only model

For $R_{0m} > 1$, there exists a unique endemic equilibrium, ϵ_{1m}^* , of the model system (4) accordingly Theorem 3. The following result deals with global asymptotic stability of ϵ_{1m}^* .

Theorem 4. For $R_{0m} > 1$, the endemic equilibrium, ϵ_{1m}^* of the model system (4) is GAS in $\Pi_m \setminus \Pi_m^0$, $\Pi_m^0 = \left\{ (S_h, E_m, I_m, R_m, S_q, I_q) : E_m = I_m = I_q = 0 \right\}$.

Proof. Consider the following candidate for a Lyapunov function which is defined on an open set, U_m^0 , containing origin: $\Gamma_m(S_h, E_m, I_m, R_m, S_q, I_q) = \frac{1}{2} \left((S_h - S_h^*) + (E_m - E_m^*) + (I_m - I_m^*) + (R_m - R_m^*) \right)^2 + \frac{1}{2} \left((S_q - S_q^*) + (I_q - I_q^*) \right)^2, \text{ with its time derivative } \frac{d\Gamma_m}{dt} = \left(S_h + E_m + I_m + R_m - (S_h^* + E_m^* + I_m^* + R_m^*) \right) \left(\frac{dS_h}{dt} + \frac{dE_m}{dt} + \frac{dI_m}{dt} + \frac{dR_m}{dt} \right) + \left(S_q + I_q - (S_q^* + I_q^*) \right) \left(\frac{dS_q}{dt} + \frac{dI_q}{dt} \right).$ (19)

It is observed that the system of equations in (14) at the disease existing equilibrium point gives,

$$\frac{\Lambda}{\mu} = S_h^* + E_m^* + I_m^* + R_m^*, \quad \frac{\Lambda_q}{\mu_q} = S_q^* + I_q^*. \tag{20}$$

Because model parameters and variables of infective classes are non-negative, combining the Eqs. (4), (5), (6), (19), (20), gives,

$$\begin{split} \frac{d\,\Gamma_m}{dt} &= \left(N_h - \frac{\Lambda}{\mu}\right)\!\left(\Lambda - \mu N_h\right) + \left(N_q - \frac{\Lambda_q}{\mu_q}\right)\!\left(\Lambda_q - \mu_q N_q\right), \\ \frac{d\,\Gamma_m}{dt} &= -\!\left(\frac{\Lambda}{\mu} - N_h\right)\!\left(\Lambda - \mu N_h\right) - \left(\frac{\Lambda_q}{\mu_q} - N_q\right)\!\left(\Lambda_q - \mu_q N_q\right), \\ &= -\!\left(\frac{\Lambda}{\mu} - N_h\right)\!\mu\!\left(\frac{\Lambda}{\mu} - N_h\right) - \left(\frac{\Lambda_q}{\mu_q} - N_q\right)\!\mu_q\!\left(\frac{\Lambda_q}{\mu_q} - N_q\right) \\ &= -\!\left[\mu\!\left(\frac{\Lambda}{\mu} - N_h\right)^2 + \mu_q\!\left(\frac{\Lambda_q}{\mu_q} - N_q\right)^2\right] < 0. \end{split}$$

As a result, $\Gamma_m' < 0$ in $\Pi_m \setminus \Pi_m^0$ when $R_{0m} > 1$. Since Γ_m is a well-defined candidate for the Lyapunov function in Π_m and by Lasalle's Invariance Principle [68], we conclude that ϵ_{1m}^* is GAS when $R_{0m} > 1$. This result indicates that every trajectory of the model (4) solutions with initial population sizes in $\Pi_m \setminus \Pi_m^0$, eventually moves towards the respective unique endemic equilibrium, ϵ_{1m}^* , of the model for $R_0 > 1$. In biological terms, the malaria infection will endure within the population as long as if $R_{0m} > 1$. \square .

Sensitivity analysis of the malaria-only model

In this section, we carry out sensitivity analysis for R_{0m} using a normalized forward sensitivity index to identify parameters that significantly influence R_{0m} . This helps in determining appropriate intervention strategies to reduce the spread of malaria. We use the method presented in [69–72] to compute the normalized forward sensitivity index of R_{0m} with respect to a given parameter p, as follows.

$$Y_p^{R_{0m}} = \frac{\partial R_{0m}}{\partial p} \times \frac{p}{R_{0m}}.$$
 (21)

The parameter values for performing sensitivity analysis of R_{0m} are provided in Table 1. Using relation (21), the sensitivity index for each parameter of R_{0m} is determined and presented in Table 2 in descending order of sensitivity, with the most sensitive parameter listed first.

Thus, it can be seen in Table 2 that the parameters β_0 , β_q , β_{hm} , Λ_q , α_m and μ have positive impact on R_{0m} . Conversely, the parameters μ_q , Λ and γ_m have negative influence on value of R_{0m} .

Table 2 Sensitivity indices of R_{0m} to parameters in malaria only model (4) using parameter values in the Table 1.

| Parameter | Value | Sensitivity index |
|--------------|-----------------------|-------------------|
| β_0 | 1 | 1 |
| μ_q | 1/15 | -1 |
| β_{hm} | 0.0044 | 0.5 |
| β_q | 0.0044 | 0.5 |
| Λ | $\mu \times N_h(0)$ | -0.5 |
| Λ_q | $\mu_q \times N_q(0)$ | 0.5 |
| γ_m | 0.00014 | -0.3908 |
| μ | 1 70×365 | 0.3905 |
| α_m | 0.0833 | 0.0002 |

For instance, if β_0 is increased or decreased by x%, then R_0 will also increase or decrease by x%. Also, decreasing value of β_{hm} by 10% would decrease value of R_{0m} by 5.1309%. In contrast, increasing value of μ_q by 10% would decrease value of R_{0m} by 4.6491%. Furthermore, based on the results in Table 2 the parameters that have a high impact on R_{0m} are; β_0 , β_{hm} , β_q and μ_q , whereas the parameter α_m has the lowest impact on it. This shows that controlling the mosquito biting rate or transmission rate among humans and infected mosquitoes will effectively reduce the spread of malaria. Also, control strategies that increase the natural mortality rates of mosquitoes will be effective in reducing the spread of the malaria epidemic in a community. Moreover, the impact of the most influencing parameters on R_{0m} is demonstrated graphically in Section "Impact of β_0 , β_{hm} , μ_q on R_{0m} ".

Leptospirosis-only model

The leptospirosis only model is obtained by setting $E_m(t) = I_m(t) = I_m(t) = R_m(t) = R_m(t) = S_a(t) = I_a(t) = 0$ in (3), given by

$$\begin{cases} \frac{dS_h}{dt} = \Lambda + \rho_l R_l - (\lambda_l + \mu) S_h, \\ \frac{dE_l}{dt} = \lambda_l S_h - (\alpha_l + \mu) E_l, \\ \frac{dI_l}{dt} = \alpha_l E_l - (\gamma_l + \mu) I_l, \\ \frac{dR_l}{dt} = \gamma_l I_l - (\rho_l + \mu) R_l, \\ \frac{dS_r}{dt} = \Lambda_r - \left(\frac{\beta_r B}{\kappa + B} + \mu_r\right) S_r, \\ \frac{dI_r}{dt} = \frac{\beta_r B}{\kappa + B} S_r - \mu_r I_r, \\ \frac{dB}{dt} = \epsilon_1 I_l + \epsilon_3 I_r - \mu_b B, \end{cases}$$

$$(22)$$

where, $\lambda_l = \frac{\beta_{he}B}{\kappa + B} + \beta_{hr}I_r$. The biologically feasible region for the model (22) is given by $\Pi_l = \left\{ (S_h, E_l, I_l, R_l, S_r, I_r, B) \in R_+^7 : N_h \leq \frac{\Lambda}{\mu}, N_r \leq \frac{\Lambda_r}{\mu_r}, B \leq \frac{\epsilon^*}{\mu_h} \left(\frac{\Lambda}{\mu} + \frac{\Lambda_r}{\mu_r} \right) \right\}, \tag{23}$

such that every solution of the system (22) starting in Π_l remain in Π_l for all $t \ge 0$ [47,50], where, $\epsilon^* = \max\{\epsilon_1, \epsilon_2\}$. Thus, the region Π_l attracts all solutions of the system (22), and it suffices to consider the dynamics of the system (22) in Π_l .

Stability of the DFE of the leptospirosis-only model

The DFE of the leptospirosis-only model system (22) is obtained by setting each of the equations of the system (22) to zero and solving for S_h and S_r . Thus, the DFE point of the system (22) is given by

$$\epsilon_{0l}^* = \left(S_h^*, 0, 0, 0, S_r^*, 0\right) = \left(\frac{\Lambda}{\mu}, 0, 0, 0, \frac{\Lambda_r}{\mu_r}, 0, 0\right). \tag{24}$$

By applying the method of the next-generation matrix [67] to the system (22), the associated basic reproduction number (R_{0l}) is derived as follows: The associated Jacobian matrices of F and V at ϵ_{0l}^* are given by

$$F = \begin{pmatrix} 0 & 0 & \frac{\beta_{hr}\Lambda}{\mu} & \frac{\beta_{he}\Lambda}{\kappa\mu} \\ 0 & 0 & 0 & 0 \\ 0 & 0 & 0 & \frac{\beta_{r}\Lambda_{r}}{\mu_{r}} \\ 0 & 0 & 0 & 0 \end{pmatrix}, \text{ and } V = \begin{pmatrix} (\alpha_{l} + \mu) & 0 & 0 & 0 \\ -\alpha_{l} & (\gamma_{l} + \mu) & 0 & 0 \\ 0 & 0 & \mu_{r} & 0 \\ 0 & -\epsilon_{1} & -\epsilon_{3} & \mu_{b} \end{pmatrix}$$

Therefore, the basic reproduction number of the leptospirosis only model (22) given by

$$R_{0l} = \rho(FV^{-1}) = \frac{1}{2} \left((R_{0lh}^e + R_{0lr}) + \sqrt{(R_{0lh}^e + R_{0lr})^2 + 4R_{0lh}^r R_{0lh}^{re}} \right), \tag{25}$$

where, $R^e_{0lh} = \frac{\beta_{he}\Lambda a_l \epsilon_1}{\kappa \mu \mu_b (a_l + \mu)(\gamma_l + \mu)}$, $R_{0lr} = \frac{\beta_r \Lambda_r \epsilon_3}{\kappa \mu_r^2 \mu_b}$, $R^r_{0lh} = \frac{\beta_{hr}\Lambda a_l}{\mu(a_l + \mu)(\gamma_l + \mu)}$, and $R^{re}_{0lh} = \frac{\beta_r \Lambda_r \epsilon_l}{\kappa \mu_r^2 \mu_b}$. According to Theorem 2 in [67], the local stability of DFE is given by the following result.

Theorem 5. The DFE, ϵ_{0l}^* , of leptospirosis-only model system (22) is locally asymptotically stable if $R_{0l} < 1$ and unstable if $R_{0l} > 1$.

Global stability of the DFE of the leptospirosis-only model

We shall use the method illustrated in [70,73,74] to investigate the global asymptotic stability (GAS) of DFE point of the model system (22). First, the model (22) should be written in the form:

$$\begin{cases} \frac{dV}{dt} = G(V, W), \\ \frac{dW}{dt} = H(V, W), H(V, 0) = 0. \end{cases}$$
(26)

where $V = (S_h, R_l, S_r)$, represents uninfected classes and $W = (E_l, I_l, I_r, B)$ denotes the infected compartments including the class of pathogens. The DFE point, ϵ_{0l}^* , of the system (22) is guaranteed to be GAS if $R_{0l} < 1$ (which is locally asymptotically stable (LAS))

and the following two conditions C_1 and C_2 hold: C_1 : For $\frac{dV}{dt} = G(V,0)$, if $V_0^* = \left(\frac{\Lambda}{\mu},0,\frac{\Lambda_r}{\mu_r}\right)$ is GAS, where, V_0^* denotes the DFE of this system. C_2 : $H(V,W) = DW - H^*(V,W), H^*(V,W) \geq 0, \forall (V,W) \in \Pi_l$, where $D = \frac{\partial H(V_0^*,0)}{\partial W}$ is a Metzler matrix. Note that $(V_0^*, 0) = \epsilon_{0l}^* = \left(\frac{\Lambda}{n}, 0, 0, 0, \frac{\Lambda_r}{n}, 0, 0\right).$

Theorem 6. The DFE, ϵ_{0l}^* , given by (24), is GAS for the model (22) if $R_{0l} < 1$.

Proof. We simply need to show that the conditions C_1 and C_2 hold provided that $R_{0l} < 1$. Substituting $E_l = I_l = I_r = B = 0$ into the system (22), yields

$$G(V,0) = \begin{pmatrix} S_h'(t) \\ R_l'(t) \\ S_r'(t) \end{pmatrix} = \begin{pmatrix} \Lambda + \rho_l R_l - \mu S_h \\ -(\rho_l + \mu) R_l \\ \Lambda_r - \mu_r S_r \end{pmatrix}, V_0^* = \begin{pmatrix} \frac{\Lambda}{\mu}, 0, \frac{\Lambda_r}{\mu_r} \end{pmatrix}. \tag{27}$$

Note that the 2nd and the 3rd equations of (27) are linear ODEs and their solutions can be easily found as:

$$R_{l}(t) = R_{l}(0)e^{-(\rho_{l} + \mu)t}, \quad S_{r}(t) = \frac{\Lambda_{r}}{\mu_{r}} \left(1 - e^{-\mu_{r}t} \right) + S_{r}(0)e^{-\mu_{r}t}. \tag{28}$$

Also, from Eqs. (27) and (28), we get

$$S'_{+}(t) = \Lambda + \sigma R_{I}(0)e^{-(\rho_{I} + \mu)t} - \mu S_{h}(t).$$
 (29)

Solving (29), gives

$$S_h(t) = \frac{\Lambda}{\mu} + S_h(0)e^{-\mu t} - R_l(0)e^{-(\rho_l + \mu)t}.$$
(30)

Now, suppose that the time, $t \to \infty$, we need to show that $V \to V_0^*$. Clearly, $R_l(t) \to 0$ and $S_r(t) \to \frac{\Lambda_r}{\mu_r}$ as $t \to \infty$, regardless of the initial population sizes $R_l(0)$ and $S_r(0)$. Thus, $S_h(t) \to \frac{\Lambda}{\mu} = N_h$, as $t \to \infty$, with the initial population size. Consequently, every point with respect to this condition converges to $V_0^* = \left(\frac{\Lambda}{u}, 0, \frac{\Lambda_r}{u}\right)$. Hence, $V_0^* = \left(\frac{\Lambda}{u}, 0, \frac{\Lambda_r}{u}\right)$ is GAS.

Next, we consider

$$H(V,W) = \begin{pmatrix} \left(\frac{\beta_{he}B}{\kappa+B} + \beta_{hr}I_r\right)S_h - (\alpha_l + \mu)E_l \\ \alpha_l E_h - (\gamma_l + \mu)I_l \\ \left(\frac{\beta_r B}{\kappa+B}\right)S_r - \mu_r I_r \\ \epsilon_1 I_l + \epsilon_2 I_r - \mu_b B \end{pmatrix}, \text{ thus, } D = \begin{pmatrix} -(\alpha_l + \mu) & 0 & \frac{\beta_{hr}A}{\mu} & \frac{\beta_{he}A}{\kappa\mu} \\ \alpha_l & -(\gamma_l + \mu) & 0 & 0 \\ 0 & 0 & -\mu_r & \frac{\beta_r A_r}{A_r \mu_r} \\ 0 & \epsilon_1 & \epsilon_2 & -\mu_b \end{pmatrix}.$$

$$(31)$$

Clearly D is a Metzler matrix, and

$$H^{\star}(V,W) = DW - H(V,W) = \begin{pmatrix} \beta_{hr}I_r\left(\frac{\Lambda}{\mu} - S_h\right) + \frac{\beta_{he}B}{\kappa}\left(\frac{\Lambda}{\mu} - \frac{\kappa}{\kappa + B}S_h\right) \\ 0 \\ \frac{\beta_rB}{\kappa}\left(\frac{\Lambda_r}{\mu_r} - \frac{\kappa}{\kappa + B}S_r\right) \\ 0 \end{pmatrix}. \tag{32}$$

Since,
$$0 \le \frac{\kappa}{\kappa + B} S_h \le S_h \le \frac{\Lambda}{\mu} \ (\because \frac{\kappa}{\kappa + B} \le 1), \ \beta_{hr} I_r \left(\frac{\Lambda}{\mu} - S_h \right) + \frac{\beta_{he} B}{\kappa} \left(\frac{\Lambda}{\mu} - \frac{\kappa}{\kappa + B_l} S_h \right) \ge 0.$$
 In the same manner, $\frac{\beta_r B}{\kappa} \left(\frac{\Lambda_r}{\mu_r} - \frac{\kappa}{\kappa + B} S_r \right) \ge 0.$

Hence, $H^{\bigstar}(V,W) \geq 0 \ \forall (V,W) \in \Pi_l$. Thus, $\epsilon_{0l}^* = \left(\frac{\Lambda}{\mu},0,0,0,\frac{\Lambda_r}{\mu_r},0,0\right)$ is GAS. Epidemiologically, it recommends that the leptospirosis infection can be eliminated from a population as long as, for $R_{0l} < 1$. Furthermore, the result shows that the system (22) has no chance of experiencing backward bifurcation at $R_{0l} = 1$ when $R_{0l} < 1$ since DFE is the only positive (stable) equilibrium point for $R_{0l} < 1$. \square

Existence of the endemic equilibrium of the leptospirosis-only model

Solving the leptospirosis-only model (22) at disease existing equilibrium denoted by $\epsilon_{ll}^* = (S_h^*, E_l^*, I_l^*, R_l^*, S_r^*, I_r^*, B^*)$, gives, Solving the leptospirosis-only model (22) at albeade existing equations $S_h^* = \frac{AJ_3 + \gamma_l \rho_l I_l^*}{J_3(\lambda_l^* + \mu)}, E_l^* = \frac{J_2}{a_l} I_l^*, R_l^* = \frac{\gamma_l}{J_3} I_l^*, S_r^* = \frac{\Lambda_r \beta_{he}}{\beta_r \Phi + \mu_r \beta_{he}},$ $I_r = \frac{\Lambda_r \beta_{he} \Phi}{\mu_r \left(\beta_r \Phi + \mu_r \beta_{he}\right)}, \quad I_l = \frac{\Lambda \alpha_l J_1 \lambda_l^* \Phi}{\mu_l J_1 J_2 J_3 + \left(J_1 J_2 J_3 - \alpha_l \rho_l \gamma_l\right) \lambda_l^*}, \quad B = \frac{1}{\mu_b} (\epsilon_1 I_l + \epsilon_3 I_r),$

$$I_r = \frac{\Lambda_r \beta_{he} \Phi}{\mu_r (\beta_r \Phi + \mu_r \beta_{he})}, \quad I_l = \frac{\Lambda \alpha_l J_1 \lambda_l^* \Phi}{\mu J_1 J_2 J_3 + (J_1 J_2 J_3 - \alpha_l \rho_l \gamma_l) \lambda_l^*}, \quad B = \frac{1}{\mu_b} (\epsilon_1 I_l + \epsilon_3 I_r), \tag{33}$$

where, $\lambda_l^* = \Phi + \beta_{hr} I_r$, $\Phi = \frac{\beta_{he}B}{\kappa + B}$, $J_1 = \alpha_l + \mu$, $J_2 = \gamma_l + \mu$, $J_3 = \rho_l + \mu$. We demonstrate the existence and local stability of the endemic equilibrium of the leptospirosis-only model based on the direction of bifurcation. The direction of bifurcation can be illustrated using the center manifold method introduced in [75]. Let us consider the following change for the variables of the system (22). Let $(S_h, E_l, I_l, R_l, S_r, I_r, B)^T = (x_1, x_2, x_3, x_4, x_5, x_6, x_7)^T = \mathbf{X}$. Thus, the system (22) can be rewritten in the form as

$$\frac{d\mathbf{X}}{dt} = F(\mathbf{X}), \text{ with } F = (f_1, f_2, f_3, f_4, f_5, f_6, f_7)^T.$$
(34)

Hence, Eq. (22) can be expressed as:

$$\begin{cases} \frac{dx_{1}}{dt} = f_{1} = \Lambda + \rho_{l}x_{4} - \left(\frac{\beta_{he}x_{7}}{\kappa + x_{7}} + \beta_{hr}x_{6} + \mu\right)x_{1}, \\ \frac{dx_{2}}{dt} = f_{2} = \left(\frac{\beta_{he}x_{7}}{\kappa + x_{7}} + \beta_{hr}x_{6}\right)x_{1} - (\alpha_{l} + \mu)x_{2}, \\ \frac{dx_{3}}{dt} = f_{3} = \alpha_{l}x_{2} - (\gamma_{l} + \mu)x_{3}, \\ \frac{dx_{4}}{dt} = f_{4} = \gamma_{l}x_{3} - (\rho_{l} + \mu)x_{4}, \\ \frac{dx_{5}}{dt} = f_{5} = \Lambda_{r} - \left(\frac{\beta_{r}x_{7}}{\kappa + x_{7}} + \mu_{r}\right)x_{5}, \\ \frac{dx_{6}}{dt} = f_{6} = \left(\frac{\beta_{r}x_{7}}{\kappa + x_{7}}\right)x_{5} - \mu_{r}x_{6}, \\ \frac{dx_{7}}{dt} = f_{7} = \epsilon_{1}x_{3} + \epsilon_{3}x_{6} - \mu_{b}x_{7}. \end{cases}$$

$$(35)$$

Taking β_{he} as bifurcation parameter and solving for $\beta_{he}=\beta_{he}^*$ at $R_{0l}=1$, from (25) gives that

$$\beta_{he}^{*} = \left[1 - \left(R_{0lh}^{e} + R_{0lr} + R_{0lh}^{r} R_{0lh}^{re}\right)\right] \frac{\kappa \mu \mu_{b}(\alpha_{l} + \mu)(\gamma_{l} + \mu)}{\Lambda \alpha_{l} \epsilon_{1}},\tag{36}$$

where, $R_{0lh}^e + R_{0lr} + R_{0lh}^r R_{0lh}^{re} = 1$ for $R_{0l} = 1$. Note that Eq. (25) satisfies

$$R_{0l}^{2} = \left(R_{0lh}^{e} + R_{0lr}\right)R_{0l} + R_{0lh}^{r}R_{0lh}^{re}, \text{ and } R_{0lh}^{e} + R_{0lr} + R_{0lh}^{r}R_{0lh}^{re} = 1, \text{ at } R_{0l} = 1.$$

$$(37)$$

The Jacobian matrix of the system (35) at $(\epsilon_{0l}^*, \beta_{he}^*)$ is obtained as

$$J(\epsilon_{0l}^*,\beta_{he}^*) = \begin{pmatrix} -\mu & 0 & 0 & \rho_l & 0 & -\frac{\beta_{hr}\Lambda}{\mu} & -\frac{\beta_{he}^*\Lambda}{\kappa\mu} \\ 0 & -J_1 & 0 & 0 & 0 & \frac{\beta_{hr}\Lambda}{\mu} & \frac{\beta_{he}^*\Lambda}{\kappa\mu} \\ 0 & \alpha_l & -J_2 & 0 & 0 & 0 & 0 \\ 0 & 0 & \gamma_l & -J_3 & 0 & 0 & 0 \\ 0 & 0 & 0 & 0 & -\mu_r & 0 & -\frac{\beta_r\Lambda_r}{\kappa\mu_r} \\ 0 & 0 & 0 & 0 & 0 & -\mu_r & \frac{\beta_r\Lambda_r}{\kappa\mu_r} \\ 0 & 0 & \epsilon_1 & 0 & 0 & \epsilon_3 & -\mu_b \end{pmatrix},$$

where, $J_1 = \alpha_l + \mu$, $J_2 = \gamma_l + \mu$, $J_3 = \rho_l + \mu$. Thus, the characteristic polynomial equation of $J(\epsilon_{0l}^*, \beta_{he}^*)$ is given by $|J(\epsilon_{0l}^*, \beta_{he}^*) - \lambda I_{7 \times 7}| = 0$ $0 \Leftrightarrow \lambda(\lambda + \mu)(\lambda + \mu_r)(\lambda + (\rho_l + \mu))(P(\lambda)) = 0$, where,

$$P(\lambda) = \lambda^3 + Q_1 \lambda^2 + Q_2 \lambda + Q_3,$$
(38)

with,

$$Q_1 = J_1 + J_2 + \mu_r + \mu_b,$$

$$\begin{split} Q_2 &= J_1(J_2 + \mu_r + \mu_b) + J_2(\mu_r + \mu_b) + \mu_r \mu_b + \frac{\beta_r \Lambda_r}{\kappa \mu_r} \epsilon_3, \\ Q_3 &= J_1 J_2 \mu_r + J_1 J_2 \mu_b + J_1 \mu_r \mu_b + J_2 \mu_r \mu_b - J_1 \frac{\beta_r \Lambda_r}{\kappa \mu_r} \epsilon_3 - \alpha_l \epsilon_1 \frac{\beta_{he}^* \Lambda}{\kappa \mu} - J_2 \frac{\beta_r \Lambda_r}{\kappa \mu_r} \epsilon_3 \\ &= J_1 J_2 \mu_r + J_1 J_2 \mu_b (1 - R_{0lh}^e) + \mu_r \mu_b (J_1 + J_2) (1 - R_{0lr}). \end{split}$$

Clearly, $\lambda_1=0, \lambda_2=-\mu, \lambda_3=-\mu_r, \lambda_4=-(\rho_l+\mu)$ are the four eigenvalues of $J(\epsilon_{0l}^*,\beta_{he}^*)$. Because each of the model parameters is non-negative, and $R_{0lh}^e<1, \ R_{0lr}<1,$ at $R_{0l}=1$, it follows that $Q_1>0, Q_2>0, Q_3>0$ and $Q_1Q_2-Q_3=J_1^2(J_2+\mu_r+\mu_b+\frac{\beta_r\Lambda_r}{\kappa\mu_r}\epsilon_3)+J_2(Q_2-\mu_r\mu_b)+(\mu_r+\mu_b)Q_2+(J_1+J_2)\frac{\beta_r\Lambda_r}{\kappa\mu_r}\epsilon_3+\alpha_l\frac{\beta_{he}^*\Lambda_r}{\kappa\mu_r}\epsilon_l>0$. Thus, by Routh's criterion, all roots of $P(\lambda)$ in (38) have negative real parts. Consequently, $J(\epsilon_{0l}^*,\beta_{he}^*)$ has a simple zero eigenvalue with all other eigenvalues having a negative real part. Therefore, the center manifold theory [76] can be used to study the dynamics of (35) near β_{he}^* . Now, following the approach in [75], $J(\epsilon_{0l}^*,\beta_{he}^*)$ has a right eigenvector corresponding to zero eigenvalue, given by $\theta=\left(\vartheta_1,\vartheta_2,\vartheta_3,\vartheta_4,\vartheta_5,\vartheta_6,\vartheta_7\right)^T$, where

$$\begin{split} & \theta_{1} = -\frac{[\mu(\alpha_{l}\gamma_{l} + J_{2}J_{3}) + \alpha_{l}J_{3}\mu]}{\mu J_{2}J_{3}} \theta_{2} < 0, \ \theta_{2} = \theta_{2} > 0, \ \theta_{3} = \frac{\alpha_{l}}{J_{2}} \theta_{2} > 0, \ \theta_{4} = \frac{\gamma_{l}}{J_{3}} \theta_{3} > 0, \\ & \theta_{5} = \frac{\beta_{r}\Lambda_{r}\alpha_{l}\epsilon_{1}}{\kappa \mu_{r}\mu^{2}J_{3}(R_{0r} - 1)} \theta_{2} < 0 \\ & (\because R_{0lr} - 1 < 0, \text{ for } R_{0l} = 1), \ \theta_{6} = -\theta_{5} > 0, \ \theta_{7} = -\frac{\kappa \mu_{r}^{2}}{\beta_{r}\Lambda_{r}} \theta_{5} > 0. \end{split}$$

Also, $J(\epsilon_{0l}^*, \beta_{he}^*)$ has a left eigenvector, $\iota = \left(\iota_1, \iota_2, \iota_3, \iota_4, \iota_5, \iota_6, \iota_7\right)^T$ associated with $\lambda = 0$, satisfying $\theta.\iota = 1$, with $\iota_1 = 0$, $\iota_2 = \iota_2 > 0$, $\iota_3 = \frac{J_1}{\alpha_l}\iota_2 > 0$, $\iota_4 = 0$, $\iota_5 = 0$, $\iota_6 = \frac{\beta_{hr}\Lambda\alpha_l\epsilon_1 + J_1J_2\mu\epsilon_3}{\alpha_l\mu\epsilon_1\mu_r}\iota_2 > 0$, $\iota_7 = \frac{J_1J_2}{\alpha_l\epsilon_1}\iota_2 > 0$.

By computing non-zero partial derivatives of f at ϵ_{0l}^* , the bifurcation constants defined by

$$a = \sum_{k,i,j=1}^{n} \iota_k \vartheta_i \vartheta_j \frac{\partial^2 f_k}{\partial x_i \partial x_j} (\epsilon_{0l}^*, \beta_{he}^*) \text{ and } b = \sum_{k,i=1}^{n} \iota_k \vartheta_i \frac{\partial^2 f_k}{\partial x_i \beta_{he}^*} (\epsilon_{0l}^*, \beta_{he}^*),$$

are given by

$$\begin{split} a &= -\frac{\iota_2 \vartheta_2^2}{J_2 \mu_b (1 - R_{0lr})} \left[\frac{\alpha_l \epsilon_1 (\beta_{hr} \beta_r + \kappa \mu_r^2) [\mu (\alpha_l \gamma_l + J_2 J_3) + \alpha_l J_3 \mu]}{\kappa \mu_b \mu_r^2 J_2 (1 - R_{0lr})} + \frac{2 \beta_{hr}^* \Lambda (\epsilon_1 \alpha_l)^2}{\kappa^2 \mu_b \mu (1 - R_{0lr})} \right. \\ &+ \frac{\beta_{hr} \Lambda \alpha_l + J_1 J_2 J_3}{\mu} + \frac{\beta_r \Lambda_r \alpha_l \epsilon_1 (\beta_r + 2 \mu_r)}{(\kappa \mu_r)^2} \left. \right] < 0, \text{ and} \\ b &= \iota_2 \vartheta_7 \frac{\partial^2 f_2}{\partial x_7 \partial \beta_{hr}^*} (\epsilon_{0l}^*, \beta_{he}^*) = \iota_2 \vartheta_7 \frac{\beta_{he}^* \Lambda}{\kappa \mu} > 0, \text{ (always)}. \end{split}$$

Based on the computed values of a < 0 and b > 0, it follows from Theorem 4.1 in [75] that the leptospirosis-only model (22) will exhibit forward bifurcation at $R_{0l} = 1$. As a result, the model's endemic equilibrium exists, is unique, and is locally and globally asymptotically stable [77,78]. This means that the disease can be eliminated from the population in the long term, if $R_{0l} < 1$. Moreover, the result for the global asymptotic stability of ϵ_{1l}^* is summarized below, with the proof provided.

Lemma 1. The unique endemic equilibrium, ϵ_{1l}^* , of the leptospirosis-only model (22) is GAS in $\Pi_l \setminus \Pi_l^0$ provided that $R_{0l} > 1$, $\Pi_l^0 = \left\{ (S_h, E_l, I_l, R_l, S_r, I_r, B) : E_l = I_l = I_r = B = 0 \right\}$.

Proof. Consider the following candidate for a Lyapunov function: $\Gamma_l(S_h, E_l, I_l, R_l, S_r, I_r, B) = \frac{1}{2} \Big((S_h - S_h^*) + (E_l - E_l^*) + (I_l - I_l^*) + (R_l - R_l^*) \Big)^2 + \frac{1}{2} \Big((S_r - S_r^*) + (I_r - I_r^*) \Big)^2 + \frac{1}{2} \Big((B_l - B_l^*)^2 + \frac{1}{2} \Big(($

$$\frac{d\Gamma_{l}}{dt} = \left(S_{h} + E_{l} + I_{l} + R_{l} - (S_{h}^{*} + E_{l}^{*} + I_{l}^{*} + R_{l}^{*})\right) \left(\frac{dS_{h}}{dt} + \frac{dE_{l}}{dt} + \frac{dI_{l}}{dt} + \frac{dR_{l}}{dt}\right) + \left(S_{r} + I_{r} - (S_{r}^{*} + I_{r}^{*})\right) \left(\frac{dS_{r}}{dt} + \frac{dI_{r}}{dt}\right) + (B - B^{*}) \frac{dB}{dt}.$$
(39)

Solving the system (22) at ϵ_{11}^* yields,

$$\frac{\Lambda}{\mu} = S_h^* + E_l^* + I_l^* + R_l^*, \quad \frac{\Lambda_r}{\mu_r} = S_r^* + I_r^*. \tag{40}$$

Since, $N_h \leq \frac{\Lambda}{\mu}$, $N_r \leq \frac{\Lambda_r}{\mu_r}$, and $B \leq \epsilon^* \left(\frac{\Lambda}{\mu} + \frac{\Lambda_r}{\mu_r}\right)$, where $\epsilon^* = \max\{\epsilon_1, \epsilon_2\}$ (see Eq. (23)), combining, the Eqs. (2), (39), (40), yields,

$$\begin{split} \frac{d\,\Gamma_l}{d\,t} &= \left(N_h - \frac{\Lambda}{\mu}\right)\!\left(\Lambda - \mu N_h\right) + \left(N_r - \frac{\Lambda_r}{\mu_r}\right)\!\left(\Lambda_r - \mu_r N_r\right) + \left[B - \epsilon^*\!\left(\frac{\Lambda}{\mu} + \frac{\Lambda_r}{\mu_r}\right)\right]\!\left[\epsilon^*\!\left(\frac{\Lambda}{\mu} + \frac{\Lambda_r}{\mu_r}\right) - B\right] \\ &= -\!\left(\frac{\Lambda}{\mu} - N_h\right)\!\mu\!\left(\frac{\Lambda}{\mu} - N_h\right) - \left(\frac{\Lambda_r}{\mu_r} - N_r\right)\!\mu_r\!\left(\frac{\Lambda_r}{\mu_r} - N_r\right) - \left[\epsilon^*\!\left(\frac{\Lambda}{\mu} + \frac{\Lambda_r}{\mu_r}\right) - B\right]\!\left[\epsilon^*\!\left(\frac{\Lambda}{\mu} + \frac{\Lambda_r}{\mu_r}\right) - B\right] \end{split}$$

Table 3 Sensitivity indices of R_{0i} to parameters in leptospirosisonly model (22) using parameter values in the Table 1.

| Parameter | Value | Sensitivity index |
|--------------|------------------------------|-------------------|
| ϵ_1 | $\log_{10}(8.1 \times 10^8)$ | 0.9987 |
| Λ | $\mu \times N_h(0)$ | 0.9987 |
| β_{he} | 0.00047 | 0.9975 |
| μ_b | 0.05 | -0.9989 |
| κ | 7000 | -0.9989 |
| γ_l | 0.0027 | -0.9846 |
| μ | 1 70×365 | -1.0260 |
| α_{l} | 0.003 | 0.0129 |
| μ_r | 0.015 | -0.0023 |
| β_r | 0.000003 | 0.0012 |
| Λ_r | 0.285 | 0.0012 |
| β_{hr} | 0.0004 | 0.001 |
| ϵ_3 | $\log_{10}(8.1 \times 10^8)$ | 0.00003427 |

$$= - \left[\mu \left(\frac{\Lambda}{\mu} - N_h \right)^2 + \mu_r \left(\frac{\Lambda_r}{\mu_r} - N_r \right)^2 \right] + \left[\left(\epsilon^* \left(\frac{\Lambda}{\mu} + \frac{\Lambda_r}{\mu_r} \right) - B \right)^2 \right] < 0.$$

As a result, $\frac{dI_l}{dt} < 0$ in $\Pi_l \setminus \Pi_l^0$ and for $R_{0l} > 1$. Since Γ_l is a well-defined candidate for the Lyapunov function, we conclude that the endemic equilibrium is GAS whenever $R_{0l} > 1$. This indicates that every trajectory of the model solutions in the long run moves towards the unique e_{1l}^* in $\Pi_l \setminus \Pi_l^0$, as $t \to \infty$.

Sensitivity analysis of the leptospirosis-only model

In this section, we perform the sensitivity analysis for R_{0l} using a normalized forward sensitivity index to determine the parameters that have a high impact on R_{0l} , which helps in providing appropriate control measures in reducing the spread of leptospirosis. Using the relation (21) the sensitivity index to each parameter of R_{0m} are given and arranged in Table 3 from the most sensitive parameter to the least sensitive.

From Table 3, we noticed that the parameters ϵ_1 , β_{he} , μ_b have the most significant influences on R_{0l} compared to others. For instance, decreasing the value of β_{he} by 15% would result in a decrease in the value of R_{0l} by 14.961%. Likewise, decreasing or increasing the value of ϵ_1 by 15% would result in a decrease or increase in the value of R_{0l} by 14.982%. In contrast, increasing the value of μ_b by 10% would decrease value of R_{0l} by 9.0788%. The sensitivity analysis of the leptospirosis-only model indicates that controlling the transmission rate among humans and contaminated environments will effectively reduce the spread of leptospirosis and leptospirosis-malaria co-infection. Also, control strategies that increase the natural removal rate of pathogens in the environment will be effective in reducing the spread of the epidemic in the community.

Malaria-leptospirosis model

The feasible region for system (3) is defined by $\Pi_{ml} = \Pi_m \times \Pi_l$, with Π_m and Π_l as specified in previous sections. Following the standard technique [47,50], it can be easily proved that every solution of the co-infection malaria-leptospirosis model (3) with non-negative initial conditions remain non-negative for all time $t \ge 0$. Moreover, every solution on the boundary of Π_{ml} eventually enter its interior [66]. Thus, Π_{ml} is positively invariant and attracts all solutions of (3) (so that, it is sufficient to study the dynamics of the system (3) in Π_{ml} .

Stability of the disease-free equilibrium malaria-leptospirosis model

The malaria -leptospirosis model (3) has a disease-free equilibrium (DFE), given by

$$\epsilon_{0ml}^* = \left(S_h^*, 0, 0, 0, 0, 0, 0, 0, S_q^*, 0, S_r^*, 0, 0\right) = \left(\frac{\Lambda}{\mu}, 0, 0, 0, 0, 0, 0, 0, 0, \frac{\Lambda_q}{\mu_q}, 0, \frac{\Lambda_r}{\mu_r}, 0, 0\right). \tag{41}$$

By applying the next-generation matrix approach (as described in previous selections a and a, the associated reproduction number for the full malaria-leptospirosis model (3) (denoted by R_{0ml}) is given by

$$R_{0ml} = \max\{R_{0m}, R_{0l}\},\tag{42}$$

where, R_{0m} the associated reproduction number for the malaria-only model (3) given in (8) and R_{0l} the associated reproduction number for the leptospirosis-only model (22) given in (25). Thus, the following result is established from Theorem 2 in [67].

Theorem 7. The DFE, ϵ_{0ml}^* , of the malaria-leptospirosis model (3) is locally asymptotically stable if $R_{0ml} < 1$ and unstable if $R_{0ml} > 1$.

Biologically, the implication of Theorem 7 is that both malaria and leptospirosis infections will die out from the population over time if $R_{0ml} < 1$ and if the initial conditions of the sub-classes of the model (3) are within the basin of attraction of ϵ_{0ml}^* . Therefore, individuals infected with malaria and leptospirosis do not get additional infections in the infected population.

Endemic equilibrium malaria-leptospirosis model

The co-existence endemic equilibrium of the full- model (3) is denoted by

 $\epsilon_{ml}^* = \left(S_h^*, E_m^*, I_m^*, E_l^*, I_l^*, I_m^*, R_m^*, R_l^*, R_{ml}^*, S_q^*, I_q^*, S_r^*, I_r^*, B^*\right)$. The explicit expression for components of ϵ_{ml}^* in terms of model parameters is not considered analytically due strong complexity of model equations. However, the model (3) has the following boundary endemic equilibria if $R_{0ml} = \max\{R_{0m}, R_{0l}\} > 1$;

- (i) $\epsilon_{ml1}^* = \left(S_{h1}^*, E_m^*, I_m^*, 0, 0, 0, R_m^*, 0, 0, S_q^*, I_q^*, 0, 0, 0\right)$ is leptospirosis free state, where expression for $S_{h1}^*, E_m^*, I_m^*, R_m^*, S_q^*$ and I_q^* are given in (15)–(17) and thus, the analysis of ϵ_{ml1}^* is similar to ϵ_{1m}^* of the model (4) described in Section "Malaria-only model".
- (ii) ε^{*}_{m/2} = (S^{*}_{h2}, 0, 0, E^{*}_l, I^{*}_l, 0, 0, R^{*}_l, 0, 0, R^{*}_l, 0, 0, 0, S^{*}_r, I^{*}_r, R^{*}_l) is malaria free state, where S^{*}_{h2}, E^{*}_l, I^{*}_l, R^{*}_l, S^{*}_r, I^{*}_r and B^{*} are given in ε^{*}_{1l} of the model (22) in Section "Leptospirosis-only model" and its analysis is similar to ε^{*}_{ll}. The steady states of both sub-models are locally and globally asymptotically stable, so the full model cannot undergo backward bifurcation, as the dynamics of the malaria-leptospirosis model are determined by those of its sub-models [50,79]. As a result, both equilibria of the model system (3) exist, and are unique, locally, and globally asymptotically stable [77,78]. Furthermore, in Section a, we demonstrate the numerical analysis of the existence and stability of DFE and the endemic equilibria of the full model.

Numerical simulations

In this section, simulations of the co-infection model (3) are performed to support the theoretical results of the model. This is accomplished in MATLAB using the *ode*45 algorithm. The model parameters used for simulations are given in Table 1, and the initial conditions are set as:

$$\left(S_h(0), E_m(0), I_m(0), E_l(0), I_l(0), I_{ml}(0), R_m(0), R_l(0), R_{ml}(0), S_q(0), I_q(0), S_r(0), I_r(0), B(0)\right) =$$
(43)

the basic reproduction number is obtained as

 $R_{0ml} = \max\{R_{0m}, R_{0l}\} \approx 2.8561 > 1$, where, $R_{0l} \approx 2.8561$ and $R_{0m} \approx 1.7229$.

Stability analysis of DFE and endemic equilibria of the full-model

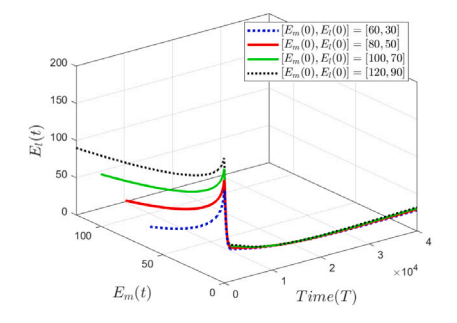
The plots in Figs. 2(a)-2(j) indicate that every solution of the malaria-leptospirosis co-infection model (3) converges to the unique endemic equilibrium, ϵ_{ml}^* , in the long run regarding the initial sizes of the sub-classes when $R_{0ml} > 1$. Thus, all infected sub-classes endure in the population. Epidemiologically, this shows that the malaria-leptospirosis co-infection will persist in the population. On the other hand, in Figs. 3(a)-3(g), we observed that every solution trajectory of the malaria-leptospirosis co-infection model (3) converges to ϵ_{0ml}^* in the long run when $R_{0ml} = \max\{0.7964, 0.9523\} = 0.9523 < 1$ with $\beta_{hr} = 0.000315$, $\beta_{he} = 0.0003$, $\beta_{r} = 0.000002$, $\beta_{hm} = 0.0034$, $\beta_{q} = 0.0034$, $\beta_{q} = 0.08$, $\gamma_{l} = 0.0035$, $\gamma_{m} = 0.00024$, $\mu_{q} = \frac{1}{14}$, $\mu_{r} = 0.02$, $\epsilon_{1} = 8.5$ and $\mu_{b} = 0.07$ and the other parameter values are used in Table 1. In Figs. 3(a)-3(d) and 3(g), all solution trajectories of (3) except trajectories of S_{h} , S_{q} and S_{r} converge to zero regardless of the initial population sizes, as $t \to \infty$, whereas $(S_{h}, S_{q}, S_{r}) \to (\frac{\Lambda}{\mu}, \frac{\Lambda_{q}}{\mu_{r}}, \frac{\Lambda_{r}}{\mu_{r}})$, as $t \to \infty$ as shown in Fig. 3(f). In biological terminology, it recommends that the malaria-leptospirosis co-infection will be eradicated from the population through time if $R_{0ml} = \max\{R_{0m}, R_{0l}\} < 1$ (if both R_{0m} and R_{0l} are less than unity).

Impact of β_0 , β_{hm} , μ_a on R_{0m}

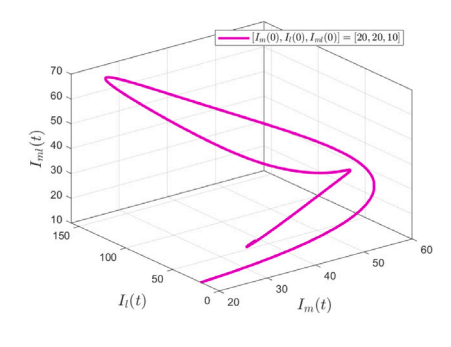
In Section "Sensitivity analysis of the malaria-only model", we discussed the sensitivity of the parameters of R_{0m} as well as the impacts of the most influencing parameters (directly or indirectly influence) on the magnitude of R_{0m} . In this section, we explore the impacts of the most sensitive parameters, β_0 , β_{hm} and μ_q on the value of R_{0m} . The graphical results are depicted in Figs. 4 and 6. In Figs. 4, 6(a) and 6(b), it can be observed that R_{0m} increases dramatically as β_0 and β_{hm} increase. In Fig. 6(a), we noticed that $R_{0m} < 1$ when $\beta_0 < 0.58$. Moreover, $R_{0m} < 1$ when $\beta_{hm} < 0.0015$ as shown in Fig. 6(b). This shows that reducing these parameter values, as indicated by the results, will sufficiently diminish the spread of malaria infection and co-infection in the community. In contrast, R_{0m} decreases steadily as μ_q increases, and $R_{0m} < 1$ when $\mu_q > \frac{1}{8.33}$ as confirmed in Fig. 6(c). This means that reducing the mosquito population plays a significant role in diminishing the number of malaria-infected individuals as well as the number of malaria-leptospirosis co-infected individuals.

Impact of β_{he} , μ_h , ϵ_1 on R_{0l}

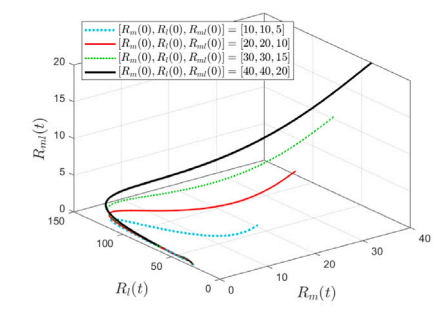
In this section, we demonstrate the impact of the most sensitive parameters β_{he} , μ_b and ϵ_1 on R_{0l} graphically. In Figs. 5, 7(a) and 7(b), it can be seen that R_{0l} increases as β_{he} , and ϵ_1 increase. On the other hand, R_{0l} decreases steadily as μ_b increases, as confirmed in Fig. 7(c). Furthermore, the value of $R_{0l} < 1$ when the value of $\beta_{he} < 0.00016$, $\epsilon_1 > 3.1$, or when $\mu_b > 0.14$, as shown in Figs. 7(a)–7(c). In biological terms, leptospirosis infection and co-infection can be eliminated from the infected population if these parameter values are less than their specified values as indicated by results.



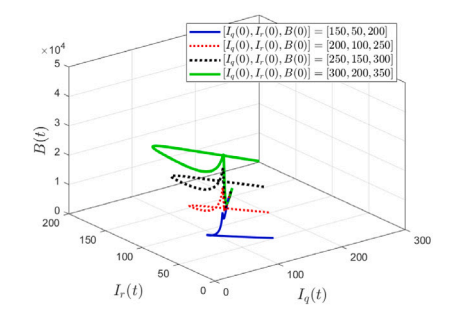
(a) Convergence of solutions of $E_m(t)$ & $E_l(t)$ with various initial values in the long run



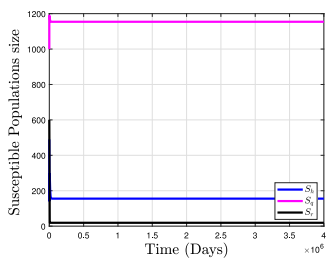
(b) Convergence of solutions of Im(t), $I_l(t)$ & $I_{ml}(t)$ with various initial values in the long run



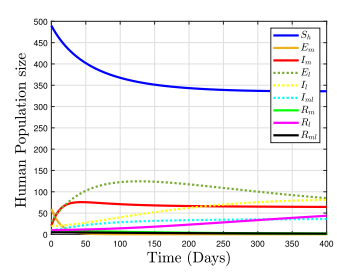
(c) Convergence of solutions of $R_m(t), R_l(t)$ & $R_{ml}(t)$ with various initial values in the long run



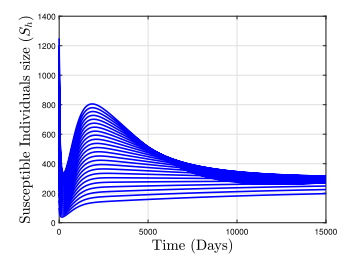
(d) Convergence of solutions of $I_q(t), I_r(t) \& B(t)$ with various initial values in the long run



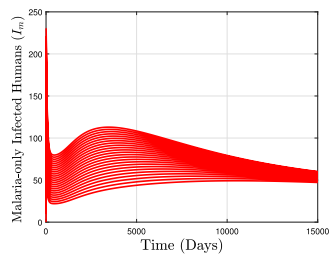
(e) Convergence of solutions of $S_h(t)$, $S_q(t)$ & $S_r(t)$ in the long run



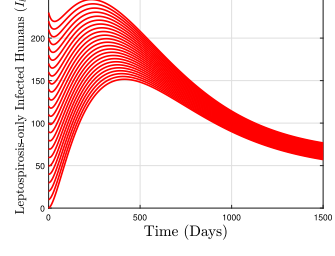
(f) The Dynamics of human populations over [0, 400]



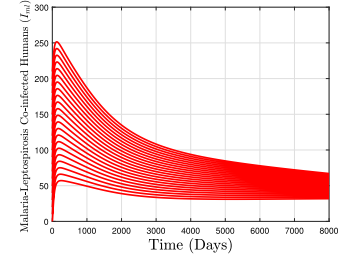
(g) Convergence of solutions of $S_h(t)$ with various initial values in the long run



(h) Convergence of solutions of $I_m(t)$ with various initial values in the long run

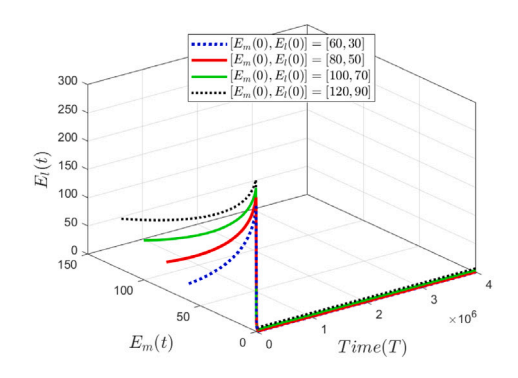


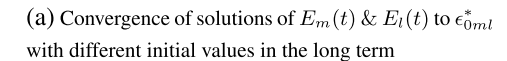
(i) Convergence of solutions of $I_l(t)$ with various initial values in the long

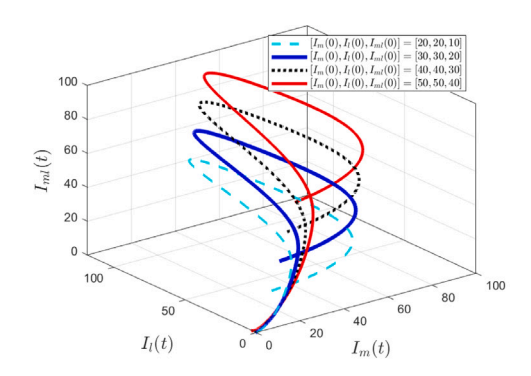


(j) Convergence of solutions of $I_{ml}(t)$ with various initial values in long run

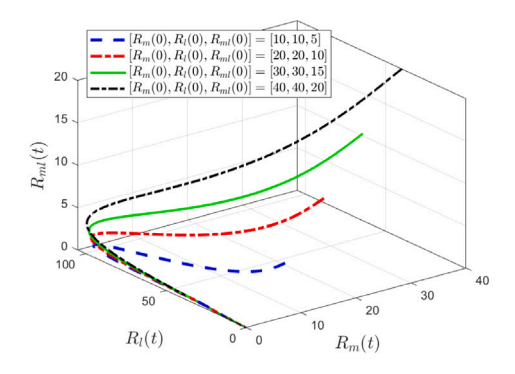
Fig. 2. Simulations of the model (3) showing convergence of solutions with different initial sizes of the sub-populations to the endemic equilibrium over time. The parameter values given in Table 1 are used (so that, $R_{0mi} \approx 2.8561 > 1$).



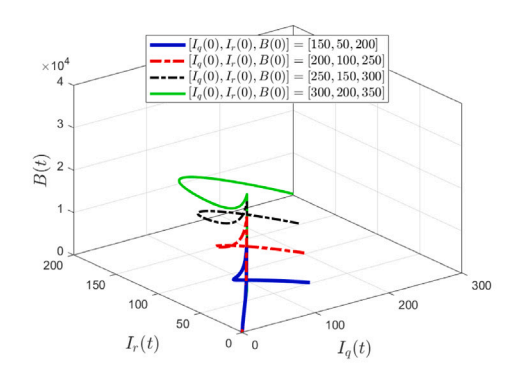




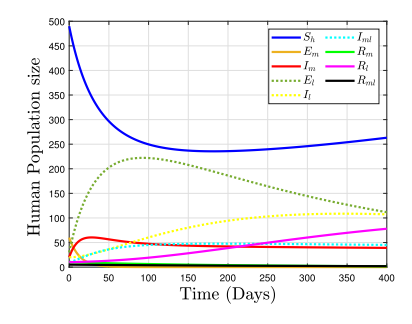
(b) Convergence of solutions of $I_m(t), I_l(t) \& I_{ml}(t)$ to ϵ_{0ml}^* with different initial values in the long term



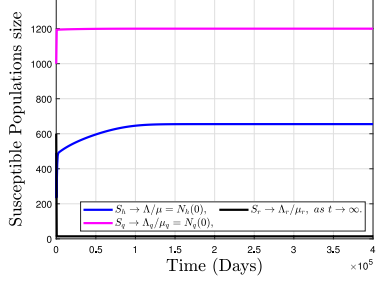
(c) Convergence of solutions of $R_m(t), R_l(t)$ & $R_{ml}(t)$ to ϵ_{0ml}^* with different initial values in the long term



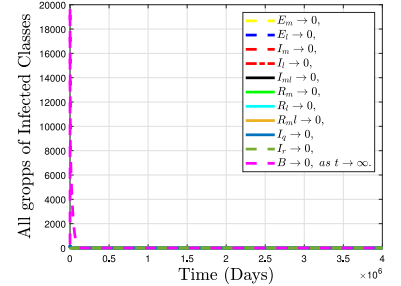
(d) Convergence of solutions of $I_q(t), I_r(t) \& B(t)$ to ϵ_{0mt}^* with different initial values in the long term



(e) The of Dynamics of the Human population over simulation period [0, 400]



(f) Convergence of solutions of susceptible humans, rodents and mosquitoes to ϵ_{0ml}^* in the long run



(g) Convergence of solutions of all infected classes to zero in the long run

Fig. 3. Simulations of the model (3) showing convergence of solutions with different initial values to the DFE, ϵ_{0ml}^* over time. The parameter values given in Table 1 are used except $\beta_{hr} = 0.000315$, $\beta_{he} = 0.0003$, $\beta_r = 0.000002$, $\beta_{hm} = 0.0034$, $\beta_q = 0.0034$, $\beta_0 = 0.8$, $\gamma_l = 0.0035$, $\gamma_m = 0.00024$, $\mu_q = \frac{1}{14}$, $\mu_r = 0.02$, $\epsilon_1 = 8.5$ and $\mu_b = 0.07$ (so that, $R_{0ml} = \max\{0.7964, 0.9523\} = 0.9523 < 1$).

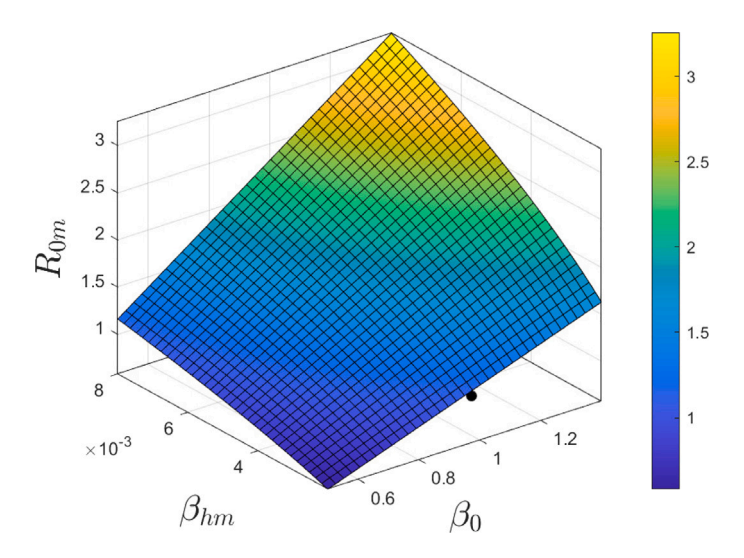


Fig. 4. Impacts of β_{hm} and β_0 on R_{0m} , for $0.002 \le \beta_{hm} \le 0.008$, $0.5 \le \beta_0 \le 1.4$. All other parameters are the same as those given in Table 1.

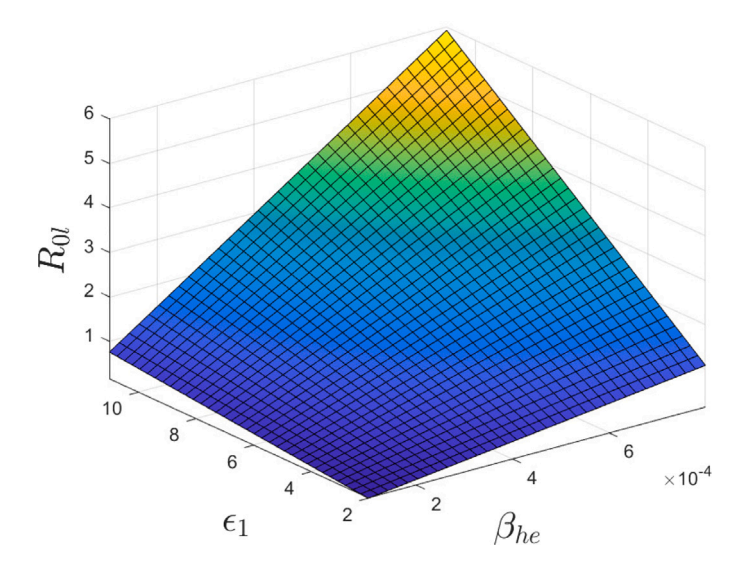


Fig. 5. Impacts of β_{he} and ϵ_1 on R_{0l} , for $0.0001 \le \beta_{he} \le 0.0008$, $2 \le \epsilon_1 \le 11$. All other parameters are the same as those given in Table 1.

Impact of β_0 on I_m , I_{ml} and I_q

In this section, the impact of β_0 on populations of infectious humans with malaria, co-infected humans, and infected mosquitoes are demonstrated in Figs. 8(a), 8(b) and 8(c), respectively. It is observed that a decrease in the values of β_0 will decrease the number of malaria-infected humans, the number of co-infected humans, and the number of infected mosquitoes steadily as shown in Figs. 8(a) – 8(c). In other words, the values of β_0 directly influence the number of infected humans and mosquitoes in these classes. This indicates that a control strategy of mosquito biting rate will sufficiently diminish the spread of malaria and malaria-leptospirosis co-infected in the community. Moreover, reducing the biting rate of mosquitoes reduces the transmission rate among humans and infected mosquitoes as well as the force of infection of humans due to infected mosquitoes. This suggests that preventive interventions, such as insecticide-treated bed nets or indoor spraying, should be provided to prevent mosquito bites, which in turn reduce the transmission of malaria in the community.

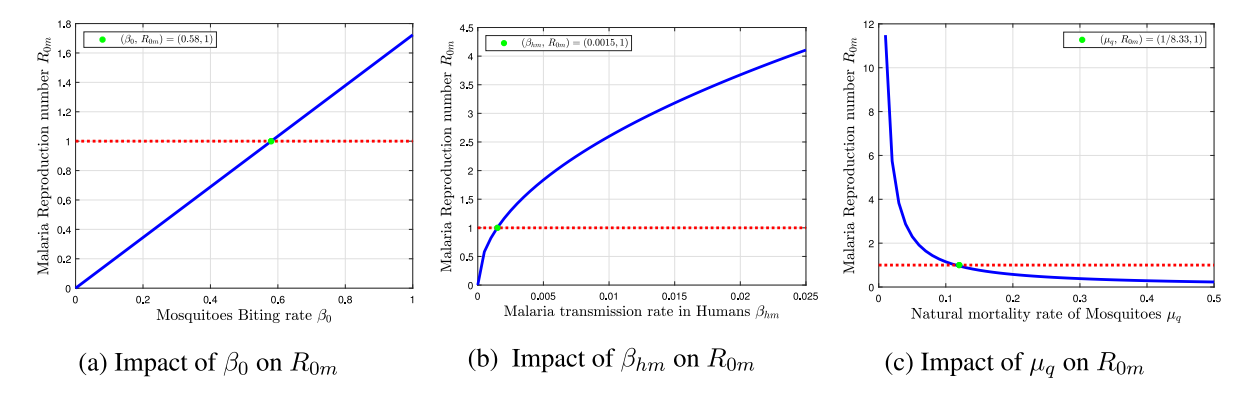


Fig. 6. Plots showing impact the most influencing parameters on R_{0m} . The parameter values given in Table 1 are used.

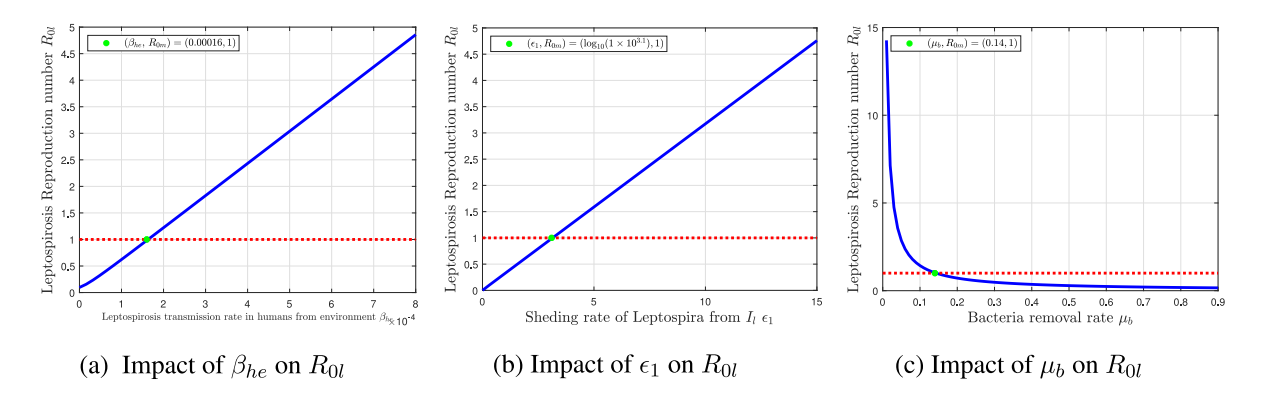


Fig. 7. Plots showing the impact of the most influencing parameters on R_{0l} . The parameter values given in Table 1 are used.

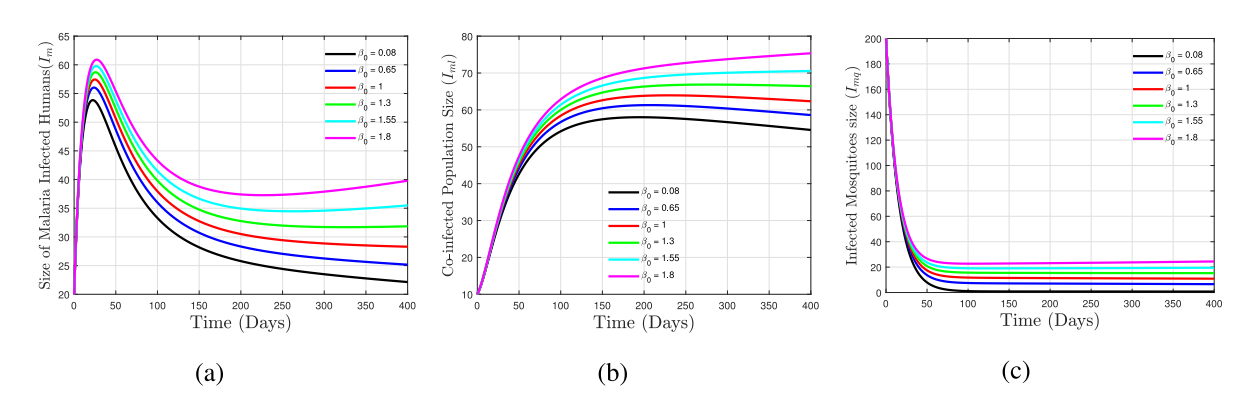


Fig. 8. Simulations of the model system (3) showing the varying effect of β_0 on the classes of; (a) infectious humans with Malaria I_m , (b) co-infected humans I_{ml} and (c) infected mosquitoes I_a .

Impact of β_{hm} on S_h , I_m and I_{ml}

In Fig. 9(a), it can be observed that decreasing β_{hm} increases the size of the susceptible individuals steadily. Thus, the number of susceptible humans getting infected in the population decreases with time. In contrast, decreasing β_{hm} decreases the number of malaria-infected individuals and the number of co-infected individuals in the population as shown in Figs. 9(b) and 9(c), respectively. This means that the malaria-infected and malaria-leptospirosis co-infected individuals can be reduced by minimizing the transmission

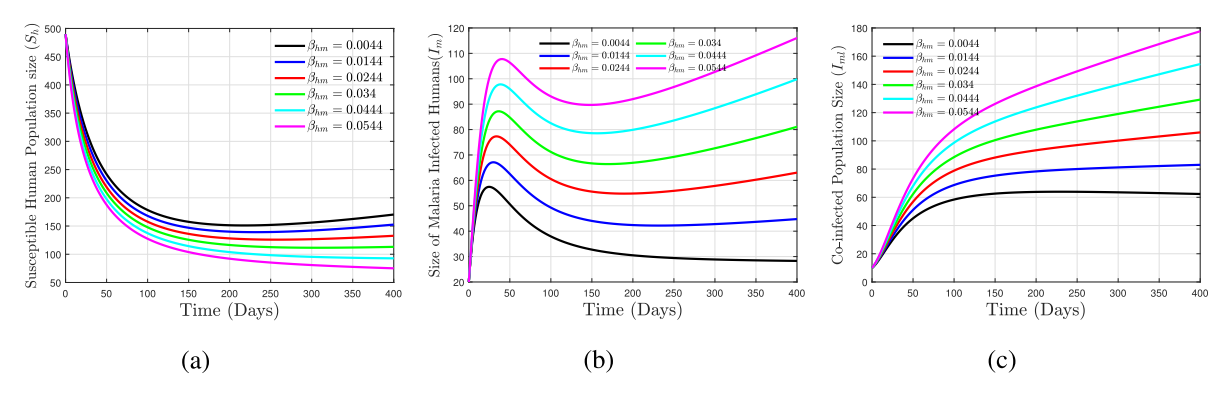


Fig. 9. Simulations of the model system (3) showing the varying effect of β_{hm} on the classes of; (a) susceptible humans S_h , (b) infectious humans with Malaria I_m and (c) co-infected humans I_{ml} .

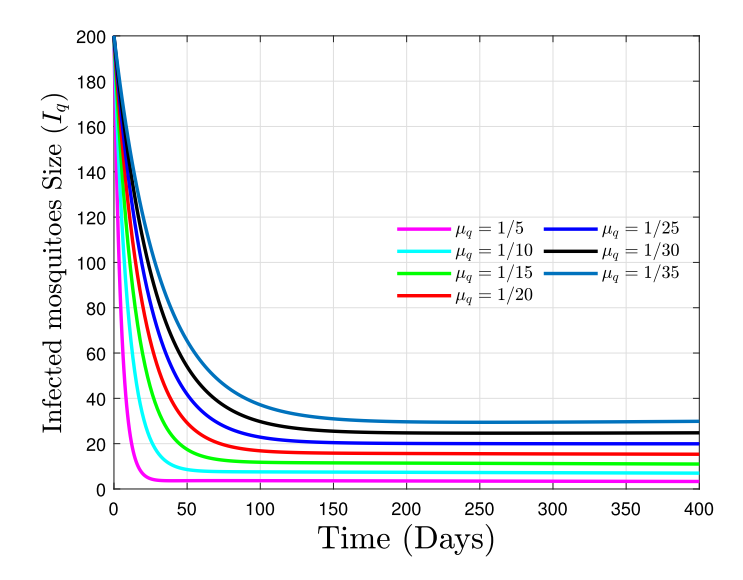


Fig. 10. Simulations of the model system (3) showing the varying effect of μ_q on population of infected mosquitoes (I_q) .

rate of humans due to infected mosquitoes. Consequently, a preventive strategy that reduces the biting of mosquitoes will sufficiently diminish the number of individuals getting infected with malaria as well as malaria-leptospirosis co-infected in the population.

Impact of μ_q on I_q

In this section, the model system (3) is simulated to demonstrate the impact of the mortality rate of mosquitoes μ_q on the infected mosquito population. It is observed in Fig. 10 that infected mosquito population decreases as μ_q increases in values. This means that a control strategy that increases the natural mortality rate of mosquitoes will effectively reduce the spread of malaria- infection. Consequently, mosquito removal strategies, like insecticide spraying, should be implemented to reduce the population of infected mosquitoes, which in turn minimizes the rate at which malaria spreads from infected mosquitoes.

Impact of ϵ_1 and μ_b on Leptospira population

In Figs. 11(a) and 11(b), it is observed that the population of the pathogen in the environment decreases steadily with time as both ϵ_1 and μ_b decrease in values. Thus, reduction of the load of *leptospira* in the environment can be achieved by improving the sanitation rate of the environment or maintaining clean surroundings, which in turn reduces the transmission rate of humans due to the e contaminated environment (β_{he}). Consequently, the number of infectious individuals with leptospirosis and co-infected individuals in the population diminishes.

Based on the numerical results shown in Figs. 6–11, we noticed that controlling human transmission rates ($\beta_{hm} \& \beta_{he}$) and enhancing removal rates of mosquitoes and bacterial populations can effectively decrease the spread of both diseases and their coinfections. This suggests that interventions targeting bacterial population reduction or mosquito biting rate control will sufficiently mitigate the spread of malaria-leptospirosis co-infection in the population. In other words, reducing the spread of mono-infections

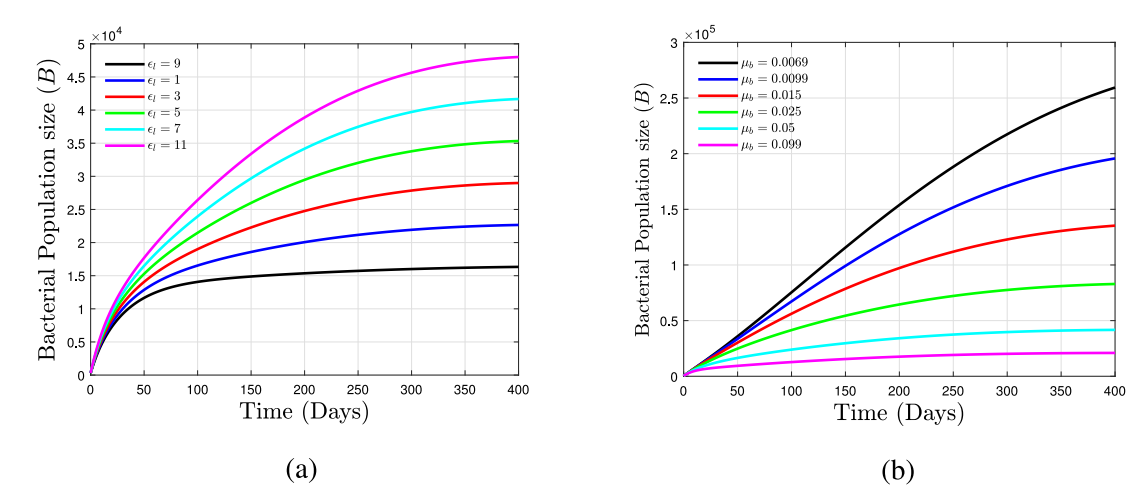


Fig. 11. Simulations of the model system (3) showing the varying effects of ϵ_1 and μ_b on B; (a) B vs ϵ_1 and (b) B vs μ_b .

and malaria-leptospirosis co-infections depends on decreasing the mosquito population and improving the sanitation rate of the environment. The effectiveness and cost-effectiveness of the suggested control measures are presented in Section a.

Optimal control analysis of the malaria-leptospirosis model

Based on the sensitivity analysis results, control measures for the parameters β_0 , β_{hm} , β_{he} , and ϵ_1 will help to sufficiently diminish the spread of malaria, leptospirosis, and malaria-leptospirosis co-infection in the population. Additionally, interventions increasing the values of μ_q and μ_b will effectively combat the spread of both diseases as well as their co-infection. In this section, we explore the autonomous malaria-leptospirosis model (3) by integrating the time-dependent controls to identify effective and cost-effective control strategies for eradicating malaria-leptospirosis co-infections. We incorporate controls $\omega_1(t)$, $\omega_2(t)$, $\omega_3(t)$ and $\omega_4(t)$ into (3) at a specified time t with $t \in [0,T]$ (T is the final time and its value is fixed), where $\omega_1(t)$: represents malaria prevention through the use of insecticide-treated bed nets and mosquito repellent lotion for skin) to prevent mosquito bites which in turn minimize the transmission of malaria within a community. $\omega_2(t)$: denotes leptospirosis prevention by using treated water for consumption and personal protective equipment like rubber boots, waterproof overalls, goggles, and gloves to diminish leptospirosis infections. $\omega_3(t)$: represents insecticide control measures for malaria such as spraying and fogging to reduce the mosquito population, we assumed that a proportional number of mosquitoes in each class of the mosquito population is removed with the constant control rate of insecticide. $\omega_4(t)$: represents the control sanitation rate of the environment; improvements in slum areas by eliminating trash, improving drainage, and environmental modifications (maintaining clean surroundings) to curb the growth of the Leptospira pathogen, and the control system is given as follows:

$$S'_{h}(t) = \Lambda + \zeta \gamma_{m} I_{m} + \rho_{m} R_{m} + \rho_{l} R_{l} + \rho_{ml} R_{ml} - \left[(1 - \omega_{1}) \lambda_{m} + (1 - \omega_{2}) \lambda_{l} + \mu \right] S_{h},$$

$$E'_{m}(t) = (1 - \omega_{1}) \lambda_{m} S_{h} - (\alpha_{m} + \mu) E_{m},$$

$$E'_{l}(t) = (1 - \omega_{2}) \lambda_{l} S_{h} - (\alpha_{l} + \mu) E_{l},$$

$$I'_{m}(t) = \alpha_{m} E_{m} + \xi_{1} \theta I_{ml} - (\gamma_{m} + \delta_{m} + \mu + \tau_{1} (1 - \omega_{2}) \lambda_{l}) I_{m},$$

$$I'_{l}(t) dt = \alpha_{l} E_{l} + \xi_{2} \theta I_{ml} - (\gamma_{l} + \delta_{l} + \mu + \tau_{2} (1 - \omega_{1}) \lambda_{m}) I_{l},$$

$$I'_{ml}(t) = \tau_{1} (1 - \omega_{2}) \lambda_{l} I_{m} + \tau_{2} (1 - \omega_{1}) \lambda_{m} I_{l} - (\theta + \mu) I_{ml},$$

$$R'_{ml}(t) = (1 - \zeta) \gamma_{m} I_{m} - (\rho_{m} + \mu) R_{m},$$

$$R'_{l}(t) = \gamma_{l} I_{l} - (\rho_{l} + \mu) R_{l},$$

$$R'_{ml}(t) = (1 - (\xi_{1} + \xi_{2})) \theta I_{ml} - (\rho_{ml} + \mu) R_{ml},$$

$$S'_{q}(t) = (1 - \omega_{3}) A_{q} - ((1 - \omega_{1}) \frac{\beta_{q} \beta_{0} (I_{m} + I_{ml})}{N_{h}} + \mu_{q} + \rho_{1} \omega_{3}) S_{q},$$

$$I'_{q}(t) = (1 - \omega_{1}) \frac{\beta_{q} \beta_{0} (I_{m} + I_{ml})}{N_{h}} S_{q} - (\mu_{q} + \rho_{1} \omega_{3}) I_{q},$$

$$S'_{r}(t) = A_{r} - (\frac{\beta_{r} B}{\kappa + B} S_{r} - \mu_{r} I_{r},$$

$$B'_{l}(t) = (1 - \omega_{2}) \varepsilon_{1} I_{l} + (1 - \omega_{2}) \varepsilon_{2} I_{ml} + \varepsilon_{3} I_{r} - (\mu_{b} + \rho_{2} \omega_{4}) B,$$

where, $\lambda_m = \frac{\beta_{hm}\beta_0 I_q}{N_h}$, $\lambda_l = \frac{\beta_{he}B}{\kappa + B} + \beta_{hr}I_r$, subject to the initial conditions: $S_h(0) \ge 0$, $E_h(0) \ge 0$, $E_h(0) \ge 0$, $I_m(0) \ge 0$,

$$O(\omega_1, \omega_2, \omega_3, \omega_4) = \int_0^{T_f} \left(y_1(I_m + I_l + I_{ml}) + y_2(S_q + I_q) + y_3 B + \frac{1}{2} \sum_{k=1}^4 Z_k \omega_k^2 \right) dt$$
 (45)

subject to the system (44), where T_f is the final time for optimal control implementation and a fixed value, the coefficients y_1, y_2 and y_3 are positive weight constants for the infectious human population (I_m , I_l and I_{ml}), total mosquito population, and the bacterial population, respectively. The terms $y_1(I_m+I_l+I_{ml})$, $y_2(S_q+I_q)$ and y_3B in the integrand O indicate the benefits of infectious humans (I_m , I_l , I_{ml}), N_q , and B. For example, selecting a high value of y_1 signifies that reducing the total number of infectious humans is more important than reducing the populations of mosquitoes and bacteria [80]. Additionally, z_1, z_2, z_3 and z_4 are positive weight constants for control functions $\omega_1, \omega_2, \omega_3$ and ω_4 , respectively. The terms $\frac{z_1}{2}\omega_1^2, \frac{z_2}{2}\omega_2^2, \frac{z_3}{2}\omega_3^2$ and $\frac{z_4}{2}\omega_4^2$ represent the cost functions associated with the malaria prevention control, leptospirosis prevention control, insecticide control for malaria and the control sanitation rate of the environment respectively. Unlike some previous works (e.g., [81–83]), we considered a linear function for the cost of infections, I_m , I_l , I_{ml} , N_q , B, and a quadratic form to represent the nonlinear costs associated with control interventions. This is consistent with the authors of various optimal control studies (see [84–87]). Justifications for selecting these cost functions are detailed in the previous studies (please refer, [88,89] and the references therein).

Our goal is to find an optimal control, $\omega^* = (\omega_1^*, \omega_2^*, \omega_3^*, \omega_4^*)$, such that

$$O(\omega_1^*, \omega_2^*, \omega_3^*, \omega_4^*) = \inf\{O(\omega_1, \omega_2, \omega_3, \omega_4) : \omega_1, \omega_2, \omega_3, \omega_4 \in \Theta\},\tag{46}$$

where, $\Theta = \{(\omega_1(t), \omega_2(t), \omega_3(t), \omega_4(t)) : 0 \le \omega_k(t) \le 1, t \in [0, T_f]\}$ is a non-empty control set and each $\omega_k(t)$ is Lebesgue measurable, k = 1, 2, 3, 4.

A Hamiltonian H, of the optimal control problem, based on PMP [90] is formulated as follows:

$$H = y_{1}(I_{m} + I_{l} + I_{ml}) + y_{2}(S_{q} + I_{q}) + y_{3}B + \frac{1}{2} \sum_{k=1}^{4} Z_{k}\omega_{k}^{2}$$

$$+ \chi_{1}S'_{h}(t) + \chi_{2}E'_{m}(t) + \chi_{3}E'_{l}(t) + \chi_{4}I'_{m}(t) + \chi_{5}I'_{l}(t) + \chi_{6}I'_{ml}(t) + \chi_{7}R'_{m}(t) + \chi_{8}R'_{l}(t)$$

$$+ \chi_{9}R'_{ml}(t) + \chi_{10}S'_{q}(t) + \chi_{11}I'_{q}(t) + \chi_{12}S'_{r}(t) + \chi_{13}I'_{r}(t) + \chi_{14}B'(t),$$

$$(47)$$

where, χ_k (k = 1, 2, ..., 14) are the adjoint variables corresponding to the state variables.

Existence of an optimal control

The following result is established for the existence of optimal controls that minimize the cost function O(45).

Theorem 8. Suppose the objective function O (45) is defined on the control set Θ subject to the optimal system (44), then there exists an optimal control quadruple $\omega^* = (\omega_1^*, \omega_2^*, \omega_3^*, \omega_3^*, \omega_4^*)$ that holds (46), provided that the following conditions given in [91] hold.

- (a) The admissible control set is closed and convex,
- (b) The right-hand-side expression of the control system (44) is bounded by a linear function in the state and control variables,
- (c) The Lagrangian of the optimal control in (45) is convex with respect to the controls,
- (d) There exist $\xi_1, \xi_2 > 0$ and $\xi_3 > 1$ such that the Lagrangian is bounded below by

$$\xi_1 \left(\sum_{k=1}^4 |\omega_k| \right)^{\frac{\xi_3}{2}} - \xi_2.$$

The proof: obviously, the control set is closed and convex by definition. Since the state and control variables have control the state system is bounded. Also, since the integrand in the equation is a finite linear combination of the state and control functions the integrand is convex with respect to control variables.

Theorem 9. Suppose $X = (S_h^*, E_m^*, I_m^*, E_l^*, I_l^*, I_l^*, R_m^*, R_l^*, R_m^*, S_q^*, I_q^*, S_r^*, I_r^*, B^*)$ is an optimal state of the state (44) and $\omega^* = (\omega_1^*, \omega_2^*, \omega_1^*, \omega_1^*, \omega_1^*, \omega_1^*)$ is an optimal control that holds (46), then there exist adjoint variables;

$$\begin{split} \chi_{1}, \chi_{2}, \chi_{3}, \chi_{4}, \chi_{5}, \chi_{6}, \chi_{7}, \chi_{8}, \chi_{9}, \chi_{10}, \chi_{11}, \chi_{12}, \chi_{13}, \chi_{14} \text{ satisfying adjoint system} \\ \chi_{1}'(t) &= (\chi_{1} - \chi_{2})(1 - \omega_{1})\lambda_{m} + (\chi_{1} - \chi_{3})(1 - \omega_{2})\lambda_{l} + \chi_{1}\mu, \\ \chi_{2}'(t) &= (\chi_{2} - \chi_{4})\alpha_{m} + \chi_{2}\mu, \\ \chi_{3}'(t) &= (\chi_{3} - \chi_{5})\alpha_{l} + \chi_{3}\mu, \\ \chi_{4}'(t) &= \chi_{4}(\gamma_{m} + \mu) + (\chi_{4} - \chi_{6})\tau_{1}(1 - \omega_{2})\lambda_{l} + (\chi_{10} - \chi_{11})(1 - \omega_{1})\frac{\beta_{q}\beta_{0}(N_{h} - I_{m})S_{q}}{(N_{h})^{2}} - \left(\chi_{1}\zeta\gamma_{m} + \chi_{7}(1 - \zeta)\gamma_{m} + y_{1}\right), \\ \chi_{5}'(t) &= \chi_{5}(\gamma_{l} + \mu) + (\chi_{5} - \chi_{6})\tau_{2}(1 - \omega_{1})\lambda_{m} - \left(\chi_{8}\gamma_{l} + \chi_{14}\epsilon_{1}(1 - \omega_{2}) + y_{1}\right), \\ \chi_{6}'(t) &= \chi_{6}(\theta + \mu) + (\chi_{10} - \chi_{11})(1 - \omega_{1})\frac{\beta_{q}\beta_{0}(N_{h} - I_{ml})S_{q}}{(N_{h})^{2}} - \left(\chi_{4}\xi_{1}\theta + \chi_{5}\xi_{2}\theta + \chi_{9}\xi_{3}\theta + \chi_{14}\epsilon_{2}(1 - \omega_{2}) + y_{1}\right), \\ \chi_{7}'(t) &= (\chi_{7} - \chi_{1})\rho_{m} + \chi_{7}\mu, \\ \chi_{8}'(t) &= (\chi_{8} - \chi_{1})\rho_{l} + \chi_{8}\mu, \\ \chi_{9}'(t) &= (\chi_{9} - \chi_{1})\rho_{ml} + \chi_{9}\mu, \\ \chi_{10}'(t) &= \chi_{10}(\mu_{q} + \varrho_{1}\omega_{3}) + (\chi_{10} - \chi_{11})(1 - \omega_{1})\frac{\beta_{q}\beta_{0}(I_{m} + I_{ml})}{N_{h}} - y_{2}, \\ \chi_{11}'(t) &= \chi_{11}(\mu_{q} + \varrho_{1}\omega_{3}) + (\chi_{1} - \chi_{2})(1 - \omega_{1})\frac{\beta_{hm}\beta_{0}S_{h}}{N_{h}} + (\chi_{5} - \chi_{6})\tau_{2}(1 - \omega_{1})\frac{\beta_{hm}\beta_{0}I_{l}}{N_{h}} - y_{2}, \\ \chi_{12}'(t) &= \chi_{12}\mu_{r} + (\chi_{12} - \chi_{13})\frac{\beta_{r}B}{\kappa + B}, \\ \chi_{13}'(t) &= (\chi_{1} - \chi_{3})(1 - \omega_{2})\beta_{hr}S_{h} + (\chi_{4} - \chi_{6})\tau_{1}(1 - \omega_{2})\beta_{hr}I_{m} + \chi_{13}\mu_{r} - \chi_{14}\epsilon_{3}, \\ \chi_{14}'(t) &= (\chi_{1} - \chi_{3})(1 - \omega_{2})\frac{\kappa\beta_{hc}S_{h}}{\kappa + B}, (\chi_{4} - \chi_{6})\tau_{1}(1 - \omega_{2})\frac{\kappa\beta_{hc}I_{m}}{(\kappa + B)^{2}} + (\chi_{12} - \chi_{13})\frac{\kappa\beta_{r}S_{r}}{(\kappa + B)^{2}} + \chi_{14}(\mu_{b} + \varrho_{2}\omega_{4}) - y_{3}, \end{split}$$

and with final time conditions,

$$\chi_k(T_f) = 0, k = 1, 2, 3, \dots, 14.$$
 (49)

Furthermore, the controls ω_i^* , i = 1, 2, 3, 4, 5 that minimizes O over Θ are given by

$$\omega_{1}^{*} = \max \left\{ 0, \min \left\{ \frac{(\chi_{2} - \chi_{1})\lambda_{m}S_{h} + (\chi_{6} - \chi_{5})\tau_{2}\lambda_{m}I_{l}}{Z_{1}}, 1 \right\} \right\}, \quad \omega_{3}^{*} = \max \left\{ 0, \min \left\{ \frac{\chi_{10}(\Lambda_{q} + \varrho_{1}S_{q}) + \chi_{11}\varrho_{1}I_{q}}{Z_{3}}, 1 \right\} \right\}, \\ \omega_{2}^{*} = \max \left\{ 0, \min \left\{ \frac{(\chi_{3} - \chi_{1})\lambda_{l}S_{h} + (\chi_{6} - \chi_{4})\tau_{1}\lambda_{l}I_{m}}{Z_{2}}, 1 \right\} \right\}, \quad \omega_{4}^{*} = \max \left\{ 0, \min \left\{ \frac{\chi_{14}\varrho_{2}B}{Z_{4}}, 1 \right\} \right\},$$

$$(50)$$

Proof. Let $X^* = (S_h^*, E_m^*, I_m^*, E_l^*, I_l^*, I_{ml}^*, R_m^*, R_l^*, R_{ml}^*, S_q^*, I_q^*, S_r^*, I_r^*, B^*)$ and $\omega^* = (\omega_1^*, \omega_2^*, \omega_3^*, \omega_4^*)$ be the optimal solutions of the optimal control problem. We apply the standard results given in PMP [92] to derive the adjoint state and the optimal control. Thus, taking negatives of partial derivatives of the Hamiltonian from (47) with respect to the associated state variables, yields the adjoint Eqs. (48):

$$\frac{\partial \dot{H}}{\partial S_{h}} = -\chi_{1}'(t), \qquad \frac{\partial H}{\partial E_{m}} = -\chi_{2}'(t), \qquad \frac{\partial H}{\partial E_{l}} = -\chi_{3}'(t), \qquad \frac{\partial H}{\partial I_{m}} = -\chi_{4}'(t), \qquad \frac{\partial H}{\partial I_{l}} = -\chi_{5}'(t),
\frac{\partial H}{\partial I_{ml}} = -\chi_{6}'(t), \qquad \frac{\partial H}{\partial R_{m}} = -\chi_{7}'(t), \qquad \frac{\partial H}{\partial R_{l}} = -\chi_{8}'(t), \qquad \frac{\partial H}{\partial R_{ml}} = -\chi_{9}'(t), \qquad \frac{\partial H}{\partial S_{q}} = -\chi_{10}'(t),
\frac{\partial H}{\partial I_{q}} = -\chi_{11}'(t), \qquad \frac{\partial H}{\partial S_{r}} = -\chi_{12}'(t), \qquad \frac{\partial H}{\partial I_{r}} = -\chi_{13}'(t), \qquad \frac{\partial H}{\partial B} = -\chi_{14}'(t), \tag{51}$$

and with transversality conditions, $\chi_k(T) = 0, k = 1, 2, \dots, 14$. Lastly, to derive optimal controls in the interior of the control set Θ , we use an optimal condition, which is given by

$$\frac{\partial H}{\partial \omega_k} = 0$$
, for ω_k^* (where $k = 1, 2, 3, 4$). (52)

Solving Eq. (52) for each optimal control gives the relation which is the same as stated in (50).

Numerical simulations and cost-effectiveness analysis of optimal control problem

In this section, we use the Forward-Backward Sweep method in the MATLAB program (details in [93]) to carry out the numerical analysis of the malaria-leptospirosis co-infection model with and without optimal controls. The aim is to demonstrate the effectiveness of various control strategies in reducing the spread of both diseases. The parameter values used in numerical simulations are given in Table 3. The initial conditions of the state variables are specified in (43). The simulation period in this numerical experiment is [0,400] in units of days. The weight constant values for human, mosquito and bacterial populations are chosen as $y_1 = 1, y_2 = 1, y_3 = 0.1$ respectively, while the weight constants for controls are $Z_1 = 10, Z_2 = 10, Z_3 = 10, Z_4 = 15$. The insecticide rate in the mosquitoes population and the control rate of treatments in infectious humans are set as $\rho_1 = 0.5$ [42] and

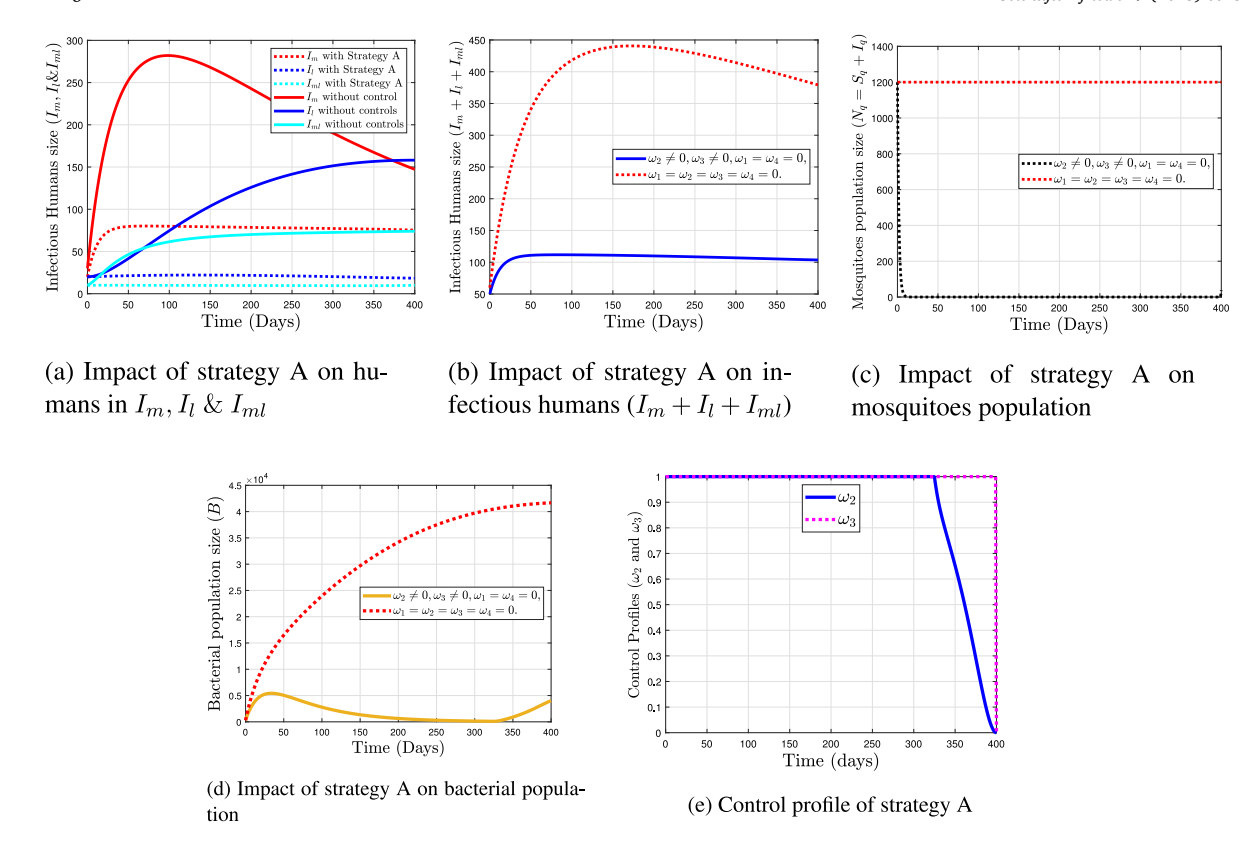


Fig. 12. Plots showing the effects of strategy A on dynamics of the malaria-leptospirosis co-infection model (44).

 $\rho_2 = 0.7$ [61]. To assess the effectiveness of optimal control strategies, we compare the following four strategies which are selected based on their effectiveness.

Strategy A: Combination of ω_2 and ω_3 ,

Strategy B: Combination of ω_1, ω_2 and ω_3 ,

Strategy C: Combination of ω_2, ω_3 and ω_4 ,

Strategy D: Combination of all controls, $\omega_1, \omega_2, \omega_3$ and ω_4 .

Case I: Optimal use of the controls ω_2 and ω_3

In this case, we implement strategy A to illustrate its impact on populations of infectious humans, mosquitoes and bacteria. The numerical results of this strategy are displayed in Figs. 12 (a) – 12 (d). Figs. 12(a) and 12(b) show a decrease in the populations of infectious humans (I_m , I_l and I_{ml}) and their total number compared to the scenario in the absence of the strategy. Similarly, this strategy plays a crucial role in diminishing the total number of mosquitoes and bacterial populations as depicted in Figs. 12 (c) and 12 (d). Additionally, Fig. 12(e) shows the control profile for this strategy, indicating that the optimal use of the control ω_2 remained at its upper bound (100%) for 324 days before decreasing to the lower limit, while the optimal usage of ω_3 was consistently at its maximum level throughout the simulation period.

Case II: Comparison of the optimal strategies B and C

In this section, we compare the effectiveness of optimal strategies B and C in reducing the populations of infectious humans, mosquitoes and bacteria. Their graphical results are demonstrated in Figs. 13 (a) – 13 (c). The figures illustrate that the total number of infectious humans ($I_m + I_l + Iml$), mosquitoes, and bacteria decrease more rapidly compared to the results in the absence of optimal controls. Both strategies effectively mitigate the total number of infectious individuals and mosquito populations. Meanwhile, in Fig. 13 (c), we observed that strategy C exhibits a higher number of pathogen removal effects from the environment compared to strategy B. In Fig. 13(d), the control profiles of strategy B suggest that the preventive efforts for malaria and leptospirosis should be kept at their maximum value for the first 5.7 and 324 days, respectively, and then gradually reduced to zero for the rest of the simulation time, while the insecticide control, ω_3 , should be sustained at its upper bound throughout the entire simulation period. Furthermore, the control profiles of strategy C are depicted in Fig. 13(e). As shown in Fig. 13(e), the control ω_2 should be sustained at the maximum effort 100% for 271 days before reducing to zero for the rest of the simulation period, whereas the control ω_3

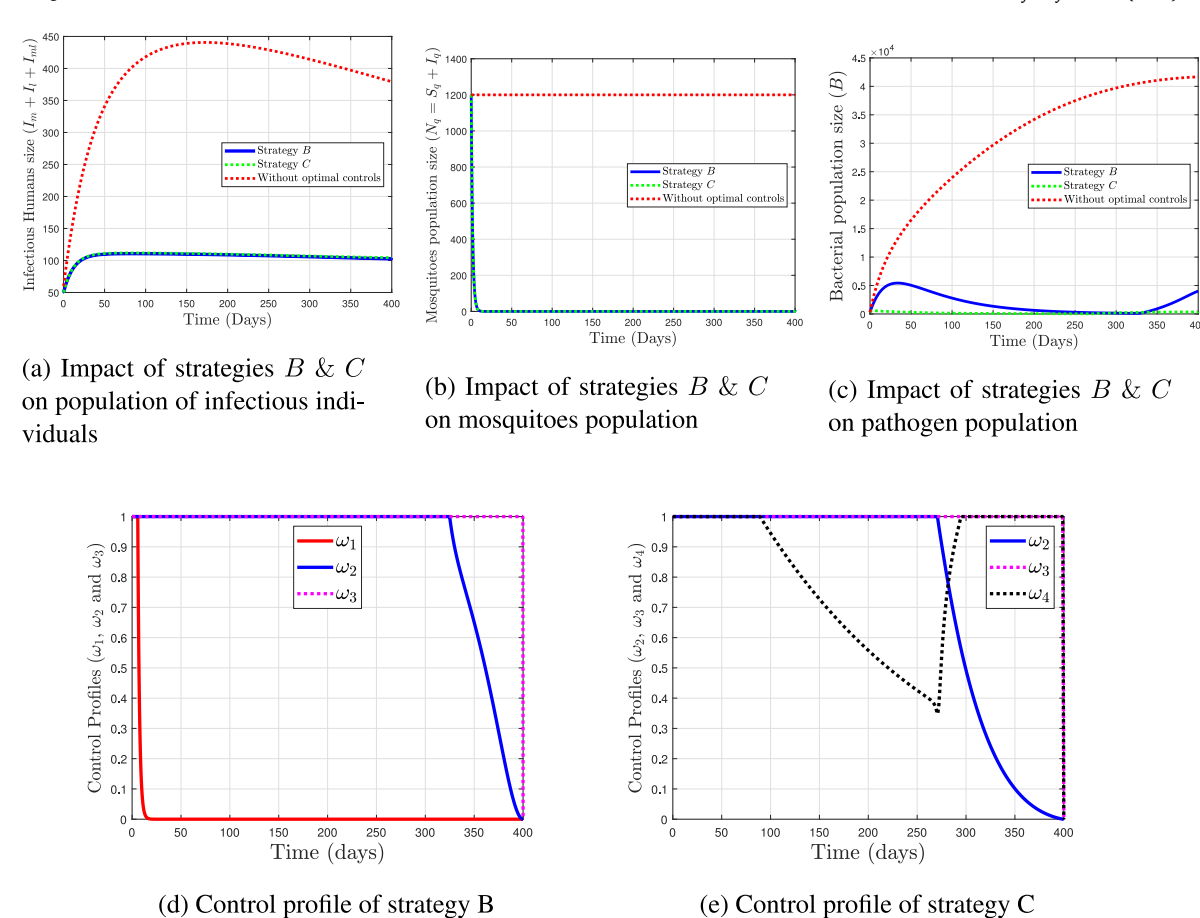


Fig. 13. Plots showing the effects of strategies B & C on dynamics of the malaria-leptospirosis co-infection model (44).

should be maintained at 100% throughout the intervention period. Meanwhile, the control ω_4 is at the maximum level for 89 days, decreases from 100% to 35.45% during the simulation period [89, 270], and then returns to 100% from [270, 295], sustained this level thereafter.

Case III: Optimal use of the all controls

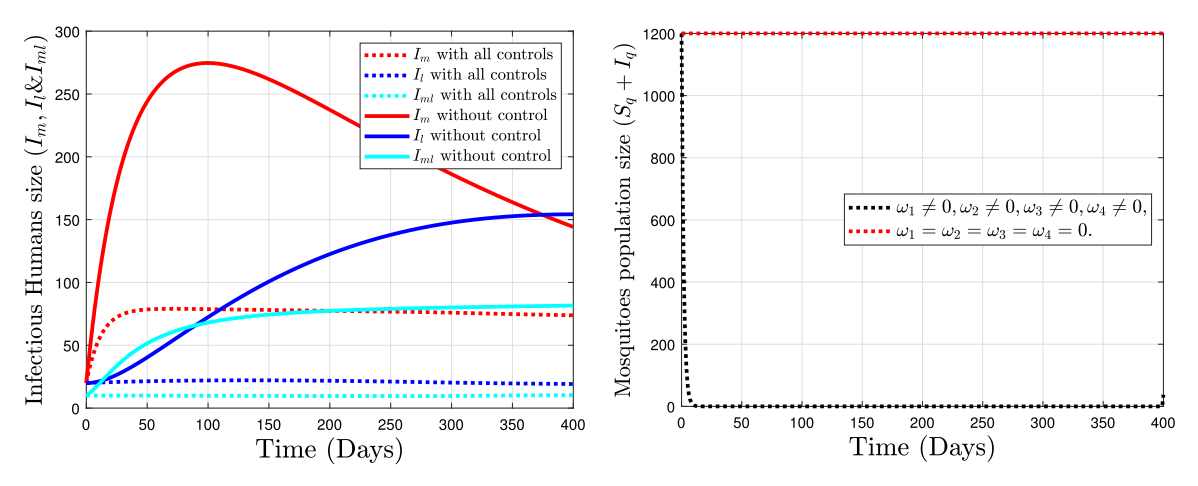
In this case, we implement strategy D, which combines all optimal controls $\omega_1, \omega_2, \omega_3$ and ω_4 to demonstrate its impact on populations of infected humans, mosquitoes, and bacteria. In Figs. 14(a)-14(c), we noticed a significant reduction in the number of infectious humans, total number of mosquitoes, and the size of the Leptospira pathogen when strategy D is implemented compared to the results without it. The control profiles of this strategy are depicted in Fig. 14(d). It is evident from Fig. 14(d) that the controls ω_1 and ω_2 maintain their maximum values for 5 and 269 days, respectively, before reducing to zero for the remainder of the simulation period. The sanitation control rate of the environment ω_4 is at maximum effort for 88 days, declines from 100% to 34.88% during the simulation period [88, 271], then rises back to 100% in the period [271, 296], sustained this level for the rest of simulation time. Meanwhile, the insecticide control, ω_3 remains at its upper value throughout the entire simulation period, as confirmed in Fig. 14(d).

Case IV: Comparison of the optimal strategies A, C and D

Based on the numerical results from case 1- case 3, we compare the effectiveness of the strategies A, C and D to determine the most effective strategy in minimizing the objective function O. The graphical illustrations can be seen in Fig. 15. It is observed from Figs. 15(a) - 15(c) and the quantitative values in Table 5 that strategy D is the most effective in minimizing the objective function $O(\omega_1, \omega_2, \omega_3, \omega_4)$ (45). Therefore, it is recommended that public health centers prioritize the implementation of strategy D, which incorporates four control measures to effectively manage and reduce the spread of mono-infections and malaria-leptospirosis co-infection in the community. The efficiency analysis and cost-effectiveness of these optimal strategies will be discussed in the subsequent sections.

Efficiency analysis

Following the works of previous studies [83,89], we perform an efficiency analysis to compare the effects of different strategies implemented in the last section using an efficiency index, denoted by Ξ . We define variable Δ as the area between the curve



- (a) Impact of strategy D on individuals in $I_m, I_l \& I_{ml}$
- (b) Impact of strategies ${\cal D}$ on mosquitoes population

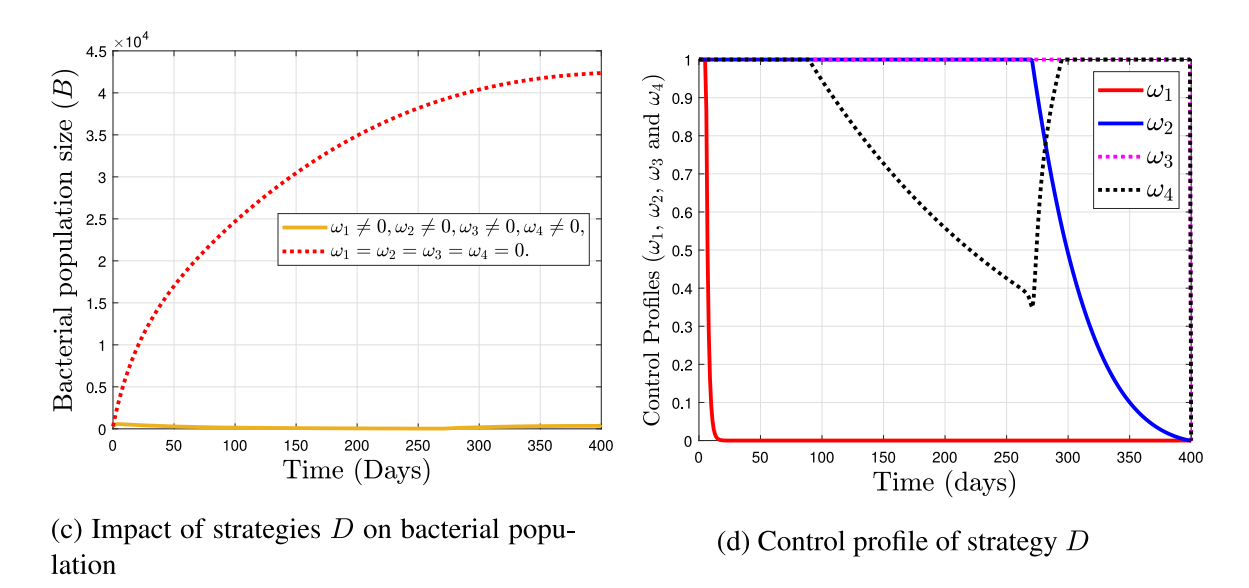


Fig. 14. Plots showing the effects of strategy D on dynamics of the malaria-leptospirosis co-infection model (44).

representing the infectious human, $I_h(I_m, I_l, I_{ml})$ population and the time over the interval $[T_0 = 0, T_f = 400]$, given by $\Delta = \int_0^{400} I_h(t) \, dt, \tag{53}$

which measures the cumulative number of infectious humans during this period. The efficiency index, Ξ , is obtained by

$$\Xi = \left(1 - \frac{\Xi_h^c}{\Xi_h^{(0)}}\right) \times 100,\tag{54}$$

where Ξ_h^c and $\Xi^{(0)}$ are, respectively, the accumulated number of infectious humans with and without control strategies. Thus, the most effective strategy will be the one with the highest efficiency index value [83,89]. The efficiency index for each of the strategies A - D is computed using the equations ((53), (54) and is given in the second column of Table 4.

Table 4 shows that strategy D is the most effective in reducing the number of infectious individuals, followed by C, A, and B, consistent with the result obtained earlier.

Remark 1. It is important to note that Δ in the second column of Table 4 represents the average accumulated number of infectious humans during the simulation period with and without control strategies and is calculated by averaging Δ_{I_m} , Δ_{I_l} and $\Delta_{I_{ml}}$. The same method is applied

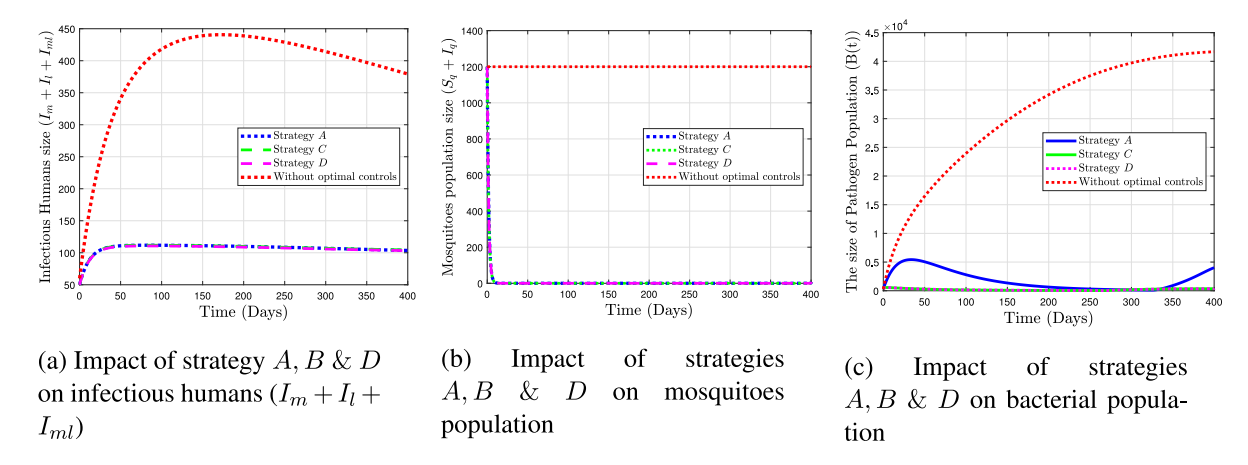


Fig. 15. Plots showing the impacts of the most effective strategies A, B & D on dynamics of the malaria-leptospirosis co-infection model (44).

| Table 4 | | | | | | |
|----------------------------|---------|--------|--|--|--|--|
| Table of efficiency index. | | | | | | |
| Strategy Δ $\Xi\%$ | | | | | | |
| No controls | 4197600 | 0 | | | | |
| A | 249 080 | 94.067 | | | | |
| В | 249 190 | 94.063 | | | | |
| C | 30 980 | 99.261 | | | | |
| D | 30 934 | 99.263 | | | | |
| | | | | | | |

for Ξ . Notably, the efficiency index values for each strategy are particularly strong, especially for strategies C and D, as we have chosen the four strategies based on their effectiveness among different possible strategies.

Cost-effectiveness analysis

In this section, we use the methods; average cost-effectiveness ratio (ACER) and the incremental cost-effectiveness ratio (ICER) in the sense of [37,94,95], to identify the most cost-effective strategy in minimizing the objective function, O.

ACER of a particular intervention strategy is given by:

$$ACER = \frac{\text{Total cost produced by a intervention strategy}}{\text{Total number of infections averted by the strategy}},$$
(55)

where, the total cost produced by a particular intervention strategy is estimated from

$$T_C = \frac{1}{2} \int_0^{T_f} \left(\sum_{k=1}^4 B_k \omega_k^2 \right) dt \tag{56}$$

and, the total number of infections averted by the strategy is estimated as the difference between the total number of infected individuals without optimal control and the total number of infected individuals with control.

The strategy with the smallest ACER value is the most cost-effective. The ACER value for the intervention strategies is calculated and presented in the 4th column of Table 5. Strategy A has the lowest ACER value, as indicated in Table 5. As a result, strategy A is the most cost-effective, followed by strategies B, C, & D, respectively. While ICER involves comparing the difference between the costs and health outcomes of any two alternative intervention strategies that are competing for the same limited resources incrementally [96–98]. ICER value of two alternative strategies is given by:

$$ICER = \frac{Change in total intervention Costs}{Change in the total number of infections averted}.$$
(57)

To implement the ICER, control strategies are ranked by the total number of infections averted total number as shown in Table 5. The strategy with the highest ICER value is discarded at each step. Additionally, Figs. 16, 17, and 18 show the total number of infections averted, the total cost of each strategy, and the average cost-effectiveness ratio. We compare intervention strategies *B* and *A* incrementally, by calculating ICER values for the two strategies as follows:

$$ICER(B) = \frac{3777.9 - 0}{3948584.6 - 0} = 0.0009568, \quad ICER(A) = \frac{3742.8 - 3777.9}{3948696.6 - 3948584.5} = -0.3134.$$
 (58)

The qualitative results obtained in Eq. (58) indicate that strategy A strongly dominates B, which implies that A is less expensive than B. As a result, strategy B is removed from the list of alternative interventions, and then strategy C is compared with strategy

Table 5
Total infections averted, total cost, ACER.

| Strategy | Infection averted (×106) | Total Cost (\$) | ACER |
|----------|--------------------------|-----------------|------------|
| В | 3.9485845 | 3777.9 | 0.0009568 |
| A | 3.9486966 | 3742.8 | 0.0009479 |
| C | 4.1667972 | 5630 | 0.00135116 |
| D | 4.1668426 | 5665.7 | 0.0013597 |

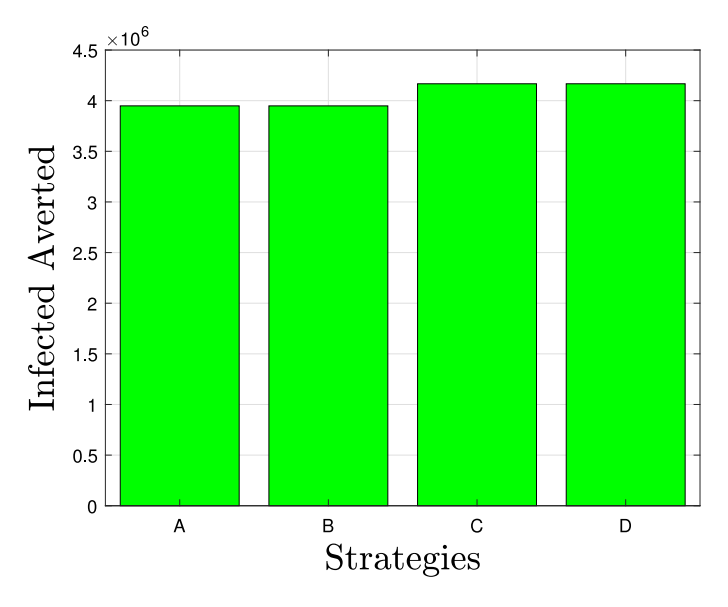


Fig. 16. Total number of infections averted for each strategy.

A as follows:

ICER(A) =
$$\frac{3742.8 - 0}{3948696.6 - 0} = 0.0009479$$
, ICER(C)= $\frac{5630 - 3742.8}{4166797.2 - 3948696.6} = 0.008653$. (59)

Based on the calculated values obtained in Eq. (59), ICER(C) is less than ICER(A). This shows that strategy C is more costly than Strategy A. Once again, strategy C is discarded from the list of alternative interventions. Consequently, strategy C is compared with strategy C incrementally.

$$ICER(A) = \frac{3742.8 - 0}{3948696.6 - 0} = 0.0009479, \quad ICER(D) = \frac{5665.7 - 3742.8}{4166842.6 - 3948696.6} = 0.008815.$$
 (60)

From Eq. (60), it is evident that ICER(D) is greater than ICER(A). This suggests that strategy A is less costly than strategy D. Thus, we concluded that strategy A is the most cost-effective among implemented intervention strategies, consistent with the result of the ACER approach obtained earlier. Therefore, public health centers and policymakers should prioritize implementing insecticide control for the mosquito population and leptospirosis preventive efforts to reduce the number of malaria and leptospirosis-infected individuals as well as malaria-leptospirosis co-infected with both diseases in the population with minimal cost.

Conclusion

In this work, we proposed and rigorously examined a new deterministic mathematical model for the dynamics of malaria-leptospirosis co-infection transmission. We also examined the optimal control problem of the malaria-leptospirosis co-infection model to assess the effectiveness of various time-dependent control measures in reducing the burden of both diseases and their co-infection. We first analyzed the sub-models of the full co-infection model associated with malaria and leptospirosis separately. The basic reproduction numbers, R_{0m} and R_{0l} associated with the malaria-only and leptospirosis-only sub-models were obtained by the technique of the next-generation matrix. Based on the construction of a suitable Lyapunov functional, the disease-free equilibrium (DFE) and endemic equilibrium of the malaria-only sub-model are globally asymptotically stable if $R_{0m} \le 1$ and $R_m > 1$, respectively. The existence, uniqueness, and global asymptotic stability of the endemic equilibrium of the leptospirosis-only sub-model for $R_{0l} > 1$ was demonstrated using the construction of a suitable Lyapunov functional and the center manifold theory, and the sub-model exhibits forward bifurcation. This result is consistent with numerous studies [50,77,78]. The results of sensitivity analysis indicated that β_0 , β_{hm} and μ_q are the most influential parameters on the value of R_{0m} , while ϵ_1 , β_{he} , μ_b are the most influential parameters on the value of R_{0l} . Based on the sub-models' results, it has been noted that the full co-infection model has unique, globally asymptotically stable DFE and endemic equilibria [50,77,79]. The global asymptotic stability of the model (3) was numerically analyzed using the

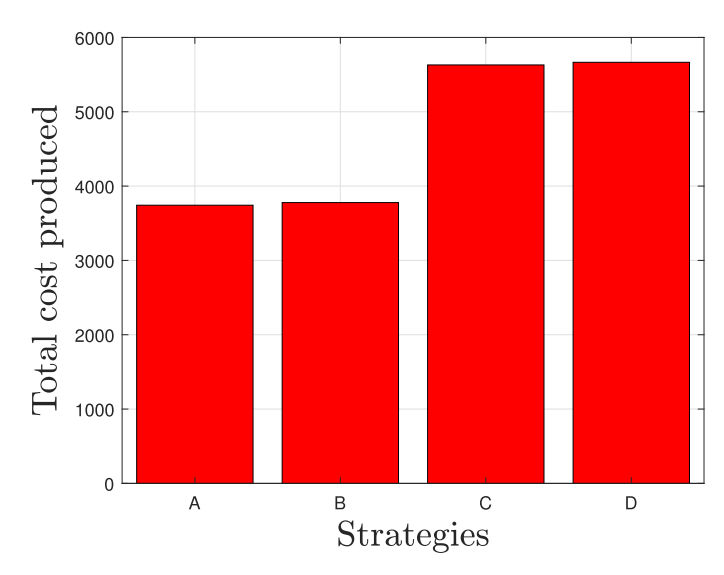


Fig. 17. Total cost for strategies.

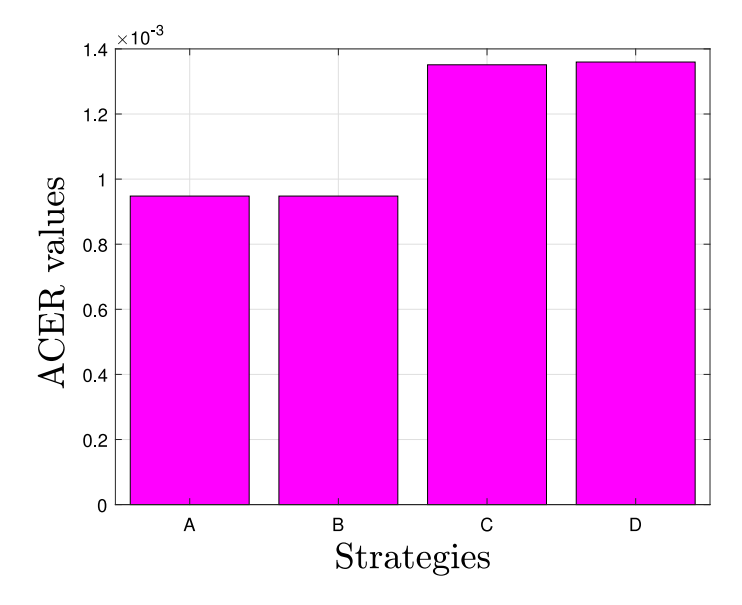


Fig. 18. ACER values for the strategies.

 ode^{45} algorithm. The graphical results of the stability analysis show that all solutions of the malaria-leptospirosis co-infection model converge toward the endemic equilibrium in the long run when $\max\{R_{0m}, R_{0l}\} \approx 2.8561 > 1$, as depicted in Fig. 2. Conversely, when R_{0ml} less than one, all model trajectories converge to the DFE of the full co-infection model, as shown in Fig. 3. This demonstrates that the co-infection of malaria-leptospirosis can be eliminated from the infected population in the long run if $R_{0ml} < 1$, whereas both diseases will persist if $R_{0ml} > 1$. Moreover, the numerical results of the uncontrolled system (3) suggest that the intervention strategies that controlling the bacterial population or reducing the biting rate of mosquitoes will sufficiently mitigate the spread of malaria-leptospirosis co-infection in the population, see Figs. 8–11. Several studies have explored mathematical models of co-infection between malaria and other diseases [47–52], identifying conditions for the occurrence of backward bifurcation. In this paper, we demonstrated that backward bifurcation does not occur in the sub-models or the malaria-leptospirosis co-infection model. Furthermore, we provided a comprehensive theoretical and numerical analysis of the global asymptotic stability of steady states of the autonomous model.

Furthermore, we explored the optimal control model of malaria-leptospirosis co-infection (44) by incorporating four timevarying control functions; $\omega_1(t)$, $\omega_2(t)$, $\omega_3(t)$, and $\omega_4(t)$. The Pontryagin maximum principle was employed to establish the necessary conditions of the optimal control problem. Numerical simulations of model (44) are carried out using an iterative method known as the forward–backwards sweep in the MATLAB program to determine the most effective optimal strategy for minimizing the objective

function. We observed that all implemented optimal strategies (A-D) effectively reduced the sizes of infectious human, mosquito, and bacterial populations compared to the autonomous system, as shown in Figs. 11–13. Additionally, each strategy had the same impact on reducing mosquito populations. However, strategy D, which implements the four optimal controls, is the most prominent in minimizing our objective function (refer to Fig. 14(a) and Fig. 13), whereas implementing the two optimal controls, ω_2 and ω_3 simultaneously (strategy A), shows to be the most cost-effective strategy. Therefore, strategy A has a significant role in reducing the spread of malaria infection, leptospirosis infection, and their co-infection in the population, particularly when available resources are limited.

CRediT authorship contribution statement

Habtamu Ayalew Engida: Conceptualization, Formal analysis, Investigation, Visualization, Validation, Data curation, Supervision, Software, Resources, Methodology, Writing – original draft, Writing – review & editing. **Demeke Fisseha:** Visualization, Validation, Resources.

Declaration of competing interest

The authors declare that they have no known competing financial interests or personal relationships that could have appeared to influence the work reported in this paper.

References

- [1] World Health Organization, Global Malaria Programme Operational Strategy 2024–2030, World Health Organization, 2024.
- [2] Dipo Aldila, Dynamical analysis on a malaria model with relapse preventive treatment and saturated fumigation, Comput. Math. Methods Med. 2022 (1) (2022) 1135452.
- [3] Tobias Mourier, Denise Anete Madureira de Alvarenga, Abhinav Kaushik, Anielle de Pina-Costa, Olga Douvropoulou, Qingtian Guan, Francisco J Guzmán-Vega, Sarah Forrester, Filipe Vieira Santos de Abreu, Cesare Bianco Júnior, et al., The genome of the zoonotic malaria parasite plasmodium simium reveals adaptations to host switching, BMC Biol. 19 (2021) 1–17.
- [4] Paul M. Sharp, Lindsey J. Plenderleith, Beatrice H. Hahn, Ape origins of human malaria, Annu. Rev. Microbiol. 74 (1) (2020) 39-63.
- [5] Victor Yman, Grace Wandell, Doreen D Mutemi, Aurelie Miglar, Muhammad Asghar, Ulf Hammar, Mattias Karlsson, Ingrid Lind, Cleis Nordfjell, Ingegerd Rooth, et al., Persistent transmission of plasmodium malariae and plasmodium ovale species in an area of declining plasmodium falciparum transmission in eastern Tanzania, PLoS Negl. Trop. Dis. 13 (5) (2019) e0007414.
- [6] Dorothy E Loy, Weimin Liu, Yingying Li, Gerald H Learn, Lindsey J Plenderleith, Sesh A Sundararaman, Paul M Sharp, Beatrice H Hahn, Out of Africa: origins and evolution of the human malaria parasites plasmodium falciparum and plasmodium vivax, Int. J. Parasitol. 47 (2–3) (2017) 87–97.
- [7] Cassidy Hill, Application of optimal control theory to a malaria model, 2021.
- [8] Diana López-Farfán, R Serge Yerbanga, Marina Parres-Mercader, Manuela Torres-Puente, Inmaculada Gómez-Navarro, Do Malick Soufiane Sanou, Adama Franck Yao, Jean Bosco Ouédraogo, Iñaki Comas, Nerea Irigoyen, et al., Prevalence of SARS-CoV-2 and co-infection with malaria during the first wave of the pandemic (the Burkina Faso case), Front. Public Heal. 10 (2022) 1048404.
- [9] Uyla Ornellas-Garcia, Patricia Cuervo, Flavia Lima Ribeiro-Gomes, Malaria and leishmaniasis: Updates on co-infection, Front. Immunol. 14 (2023) 1122411.
- [10] World Health Organization, et al., World Malaria Report 2022, World Health Organization, 2022.
- [11] World Health Organization, World Malaria Report 2023, World Health Organization, 2023.
- [12] Colleen L Lau, Nicola Townell, Eloise Stephenson, Scott B Craig, Leptospirosis: An important zoonosis acquired through work, play and travel, Aust. J. Gen. Pract. 47 (3) (2018) 105–110.
- [13] Leon Biscornet, Christophe Révillion, Sylvaine Jégo, Erwan Lagadec, Yann Gomard, Gildas Le Minter, Gérard Rocamora, Vanina Guernier-Cambert, Julien Mélade, Koussay Dellagi, et al., Predicting the presence of leptospires in rodents from environmental indicators opens up opportunities for environmental monitoring of human leptospirosis, Remote Sens. 13 (2) (2021) 325.
- [14] Daniel Stephen Masunga, Anushree Rai, Mortada Abbass, Olivier Uwishema, Jack Wellington, Lama Uweis, Rayyan El Saleh, Sara Arab, Chinyere Vivian Patrick Onyeaka, Helen Onyeaka, Leptospirosis outbreak in Tanzania: an alarming situation, Ann. Med. Surg. 80 (2022) 104347.
- [15] Maysa Pellizzaro, Camila Marinelli Martins, Ana Carolina Yamakawa, Diogo da Cunha Ferraz, Vivien Midori Morikawa, Fernando Ferreira, Andrea Pires dos Santos, Alexander Welker Biondo, Helio Langoni, Molecular detection of leptospira spp. in rats as early spatial predictor for human disease in an endemic urban area, PLoS One 14 (5) (2019) e0216830.
- [16] Kenneth Boey, Kanae Shiokawa, Sreekumari Rajeev, Leptospira infection in rats: A literature review of global prevalence and distribution, PLoS Negl. Trop. Dis. 13 (8) (2019) e0007499.
- [17] Bart J. Currie, Mirjam Kaestli, A global picture of melioidosis, Nature 529 (7586) (2016) 290-291.
- [18] Mohammad R Mohd Ali, Amira W Mohamad Safiee, Padmaloseni Thangarajah, Mohd H Fauzi, Alwi Muhd Besari, Nabilah Ismail, Chan Yean, Molecular detection of leptospirosis and melioidosis co-infection: a case report, J. Infect. Public Heal. 10 (6) (2017) 894–896.
- [19] Collins Chimezie Udechukwu, Caleb Ayuba Kudi, Paul Ayuba Abdu, Elmina Abiba Abiayi, Ochuko Orakpoghenor, Prevalence of leptospira interrogans in wild rats (Rattus norvegicus and Cricetomys gambianus) in Zaria, Nigeria, Heliyon 7 (1) (2021) e05950.
- [20] Kanokwan Suwannarong, Ngamphol Soonthornworasiri, Pannamas Maneekan, Surapon Yimsamran, Karnsunaphat Balthip, Santi Maneewatchararangsri, Watcharee Saisongkorh, Chutarat Saengkul, Suntaree Sangmukdanun, Nittaya Phunta, et al., Rodent-human interface: Behavioral risk factors and leptospirosis in a province in the central region of Thailand, Vet. Sci. 9 (2) (2022) 85.
- [21] Vannarat Saechan, Daraka Tongthainan, Wirasak Fungfuang, Phitsanu Tulayakul, Gittiyaporn Ieamsaard, Ruttayaporn Ngasaman, Natural infection of leptospirosis and melioidosis in long-tailed macaques (Macaca fascicularis) in Thailand, J. Vet. Med. Sci. 84 (5) (2022) 700–706.
- [22] CDC Leptospirosis, Fact sheet for clinicians, Centers Dis. Control. Prev. (2018).
- [23] S.J. Khan, M.B. Khattak, A. Khan, Leptospirosis: a disease with global prevalence, J. Microbiol. Exp. 6 (5) (2018) 219-221.
- [24] Amélie Desvars-Larrive, Steve Smith, Gopi Munimanda, Pascale Bourhy, Theresa Waigner, Margaret Odom, Diana S Gliga, Chris Walzer, Prevalence and risk factors of leptospira infection in urban brown rats (Rattus norvegicus), Vienna, Austria, Urban Ecosyst. 23 (4) (2020) 775–784.
- [25] Mayowa M Ojo, Olumuyiwa James Peter, Emile Franc Doungmo Goufo, Kottakkaran Sooppy Nisar, A mathematical model for the co-dynamics of COVID-19 and tuberculosis, Math. Comput. Simulation 207 (2023) 499–520.
- [26] Maia Martcheva, vol. 61, Springer, 2015, pp. 1-32.

[27] Axel O.G. Hoarau, Patrick Mavingui, Camille Lebarbenchon, Coinfections in wildlife: Focus on a neglected aspect of infectious disease epidemiology, PLoS Pathog. 16 (9) (2020) e1008790.

- [28] Polrat Wilairatana, Wanida Mala, Pongruj Rattaprasert, Kwuntida Uthaisar Kotepui, Manas Kotepui, Prevalence of malaria and leptospirosis co-infection among febrile patients: A systematic review and meta-analysis, Trop. Med. Infect. Dis. 6 (3) (2021) 122.
- [29] Asmalia Md-Lasim, Farah Shafawati Mohd-Taib, Mardani Abdul-Halim, Ahmad Mohiddin Mohd-Ngesom, Sheila Nathan, Shukor Md-Nor, Leptospirosis and coinfection: should we be concerned? Int. J. Environ. Res. Public Heal. 18 (17) (2021) 9411.
- [30] Mohan Rao, Nurul Atiqah, Mukmina Dasiman, Fairuz Amran, Demographic, clinical and laboratory features of leptospirosis-malaria co-infections in peninsular Malaysia, J. Med. Microbiol. 69 (3) (2020) 451–456.
- [31] Krishna Venkatesh Baliga, Yanamandra Uday, Vivek Sood, Akhil Nagpal, Acute febrile hepato-renal dysfunction in the tropics: co-infection of malaria and leptospirosis, J. Infect. Chemother. 17 (2011) 694–697.
- [32] Mohan Gurjar, Saurabh Saigal, Arvind K Baronia, Afzal Azim, Banani Poddar, Ratender K Singh, Clinical manifestations of co-infection with malaria and leptospirosis, Trop. Dr. 41 (3) (2011) 175–178.
- [33] Sukhen Samanta, Sujay Samanta, Rudrashish Haldar, Emergency caesarean delivery in a patient with cerebral malaria-leptospira co infection: Anaesthetic and critical care considerations, Indian J. Anaesth. 58 (1) (2014) 55.
- [34] Yi Xie, Ziheng Zhang, Yan Wu, Shuang Li, Liuyong Pang, Yong Li, Time-delay dynamic model and cost-effectiveness analysis of major emergent infectious diseases with transportation-related infection and entry-exit screening, Math. 12 (13) (2024) 2069.
- [35] Habtamu Ayalew Engida, Duncan Kioi Gathungu, Melkamu Molla Ferede, Malede Atnaw Belay, Patiene Chouop Kawe, Bilali Mataru, Optimal control and cost-effectiveness analysis for the human melioidosis model, Heliyon 10 (4) (2024).
- [36] Mo'tassem Al-arydah, Hailay Berhe, Khalid Dib, Kalyanasundaram Madhu, Mathematical modeling of the spread of the coronavirus under strict social restrictions, Math. Methods Appl. Sci. (2021).
- [37] Mini Ghosh, Samson Olaniyi, Olawale S. Obabiyi, Mathematical analysis of reinfection and relapse in malaria dynamics, Appl. Math. Comput. 373 (2020) 125044.
- [38] Zhihong Zhao, Shaochun Li, Yulan Lu, Mathematical Models for the Transmission of Malaria with Seasonality and Ivermectin, Texas State University, Department of Mathematics, 2022.
- [39] O.C. Collins, K.J. Duffy, A mathematical model for the dynamics and control of malaria in Nigeria, Infect. Dis. Model. 7 (4) (2022) 728-741.
- [40] Robert Smith Mo'tassem Al-Arydah, et al., Controlling malaria with indoor residual spraying in spatially heterogenous environments, Math. Biosci. Eng. 8 (4) (2011) 889-914.
- [41] Dipo Aldila, Michellyn Angelina, Optimal control problem and backward bifurcation on malaria transmission with vector bias, Heliyon 7 (4) (2021).
- [42] Faishal Farrel Herdicho, Williams Chukwu, Hengki Tasman, et al., An optimal control of malaria transmission model with mosquito seasonal factor, Results Phys. 25 (2021) 104238.
- [43] Stephane Y Tchoumi, CW Chukwu, ML Diagne, H Rwezaura, ML Juga, JM Tchuenche, Optimal control of a two-group malaria transmission model with vaccination, Netw. Model. Anal. Heal. Informatics Bioinform. 12 (1) (2022) 7.
- [44] Hengki Tasman, Dipo Aldila, Putri A Dumbela, Meksianis Z Ndii, Fatmawati, Faishal F Herdicho, Chidozie W Chukwu, Assessing the impact of relapse, reinfection and recrudescence on malaria eradication policy: a bifurcation and optimal control analysis, Trop. Med. Infect. Dis. 7 (10) (2022) 263.
- [45] Bevina D Handari, Rossi A Ramadhani, Chidozie W Chukwu, Sarbaz HA Khoshnaw, Dipo Aldila, An optimal control model to understand the potential impact of the new vaccine and transmission-blocking drugs for malaria: A case study in Papua and West Papua, Indonesia, Vaccines 10 (8) (2022) 1174.
- [46] Iffatricia Haura Febiriana, Abdullah Hasan Hassan, Dipo Aldila, Enhancing malaria control strategy: Optimal control and cost-effectiveness analysis on the impact of vector bias on the efficacy of mosquito repellent and hospitalization, J. Appl. Math. 2024 (1) (2024) 9943698.
- [47] Zindoga Mukandavire, Abba B Gumel, Winston Garira, Jean Michel Tchuenche, Mathematical analysis of a model for HIV-malaria co-infection, 2009.
- [48] K.O. Okosun, Oluwole Daniel Makinde, A co-infection model of malaria and cholera diseases with optimal control, Math. Biosci. 258 (2014) 19-32.
- [49] Folashade B. Agusto, Ibrahim M. ELmojtaba, Optimal control and cost-effective analysis of malaria/visceral leishmaniasis co-infection, PLoS One 12 (2) (2017) e0171102.
- [50] S.Y. Tchoumi, M.L. Diagne, H. Rwezaura, J.M. Tchuenche, Malaria and COVID-19 co-dynamics: A mathematical model and optimal control, Appl. Math. Model. 99 (2021) 294–327.
- [51] Ahmed M. Elaiw, Afnan D. Al Agha, Global stability of a reaction-diffusion malaria/COVID-19 coinfection dynamics model, Math. 10 (22) (2022) 4390.
- [52] A.D.A. Agha, A.M. Elaiw, Global dynamics of SARS-CoV-2/malaria model with antibody immune response, Math. Biosci. Eng.: MBE 19 (8) (2022)
- [53] Haileyesus Tessema Alemneh, A co-infection model of dengue and leptospirosis diseases, Adv. Difference Equ. 2020 (1) (2020) 664.
- [54] Muhammad Altaf Khan, Saeed Islam, Sher Afzal Khan, Mathematical modeling towards the dynamical interaction of leptospirosis, Appl. Math. Inf. Sci. 8 (3) (2014) 1049.
- [55] Muhammad Altaf Khan, Syed Farasat Saddiq, Saeed Islam, Ilyas Khan, Sharidan Shafie, Dynamic behavior of leptospirosis disease with saturated incidence rate. Int. J. Appl. Comput. Math. 2 (4) (2016) 435–452.
- [56] Abhineshwary Bhalraj, Amirah Azmi, Mathematical modelling of the spread of leptospirosis, in: AIP Conference Proceedings, vol. 2184, (1) AIP Publishing LLC. 2019. 060031.
- [57] Habtanu Ayalew Engida, David Mwangi Theuri, Duncan Gathungu, John Gachohi, Haileyesus Tessema Alemneh, A mathematical model analysis for the
- transmission dynamics of leptospirosis disease in human and rodent populations, Comput. Math. Methods Med. (2022). [58] Kazeem Oare Okosun, M. Mukamuri, Daniel Oluwole Makinde, Global stability analysis and control of leptospirosis, Open Math. 14 (1) (2016) 567–585.
- [59] Amanda Minter, Federico Costa, Hussein Khalil, Jamie Childs, Peter Diggle, Albert I Ko, Mike Begon, Optimal control of rat-borne leptospirosis in an urban environment, Front. Ecol. Evol. 7 (2019) 209.
- [60] Ratchaneewan Paisanwarakiat, Rinrada Thamchai, Optimal control of a leptospirosis epidemic model, Sci. Technol. Asia (2021) 9-17.
- [61] Habtamu Ayalew Engida, David Mwangi Theuri, Duncan Kioi Gathungu, John Gachohi, Optimal control and cost-effectiveness analysis for leptospirosis epidemic, J. Biol. Dyn. 17 (1) (2023) 2248178.
- [62] Gbenga Adegbite, Sunday Edeki, Itunuoluwa Isewon, Jerry Emmanuel, Titilope Dokunmu, Solomon Rotimi, Jelili Oyelade, Ezekiel Adebiyi, Mathematical modeling of malaria transmission dynamics in humans with mobility and control states, Infect. Dis. Model. 8 (4) (2023) 1015–1031.
- [63] Gbenga J. Abiodun, P. Witbooi, Kazeem O. Okosun, Modelling the impact of climatic variables on malaria transmission, Hacet. J. Math. Stat. 47 (2) (2018) 219–235.
- [64] Kamaldeen Okuneye, Abba B. Gumel, Analysis of a temperature-and rainfall-dependent model for malaria transmission dynamics, Math. Biosci. 287 (2017) 72–92.
- [65] S Olaniyi, OD Falowo, KO Okosun, M Mukamuri, OS Obabiyi, OA Adepoju, Effect of saturated treatment on malaria spread with optimal intervention, Alex. Eng. J. 65 (2023) 443–459.
- [66] Vivian Hutson, Klaus Schmitt, Permanence and the dynamics of biological systems, Math. Biosci. 111 (1) (1992) 1-71.
- [67] Pauline Van den Driessche, James Watmough, Reproduction numbers and sub-threshold endemic equilibria for compartmental models of disease transmission, Math. Biosci. 180 (1–2) (2002) 29–48.
- [68] Joseph P. La Salle, The Stability of Dynamical Systems, SIAM, 1976.

[69] Nakul Chitnis, James M. Hyman, Jim M. Cushing, Determining important parameters in the spread of malaria through the sensitivity analysis of a mathematical model, Bull. Math. Biol. 70 (2008) 1272–1296.

- [70] Habtamu Ayalew Engida, David Mwangi Theuri, Duncan Gathungu, John Gachohi, Haileyesus Tessema Alemneh, A mathematical model analysis of the human melioidosis transmission dynamics with an asymptomatic case, Heliyon (2022) e11720.
- [71] Hailay Weldegiorgis Berhe, Abadi Abay Gebremeskel, Zinabu Teka Melese, Asdenaki Aklilu Gebremichael, et al., Modeling and global stability analysis of COVID-19 dynamics with optimal control and cost-effectiveness analysis, Partial. Differ. Equ. Appl. Math. 11 (2024) 100843.
- [72] Mo'tassem Al-arydah, Robert Smith?, Adding education to "test and treat": can we overcome drug resistance? J. Appl. Math. 2015 (1) (2015) 781270.
- [73] C. Castillo Chavez, Z. Feng, W. Huang, On the computation of R0 and its role on global stability, Math. Approaches Emerg. Re-Emerging Infect. Dis.: Introd. 125 (2002) 31–65.
- [74] A. Omame, C.U. Nnanna, S.C. Inyama, Optimal control and cost-effectiveness analysis of an HPV-chlamydia trachomatis co-infection model, Acta Biotheor. 69 (2021) 185–223.
- [75] Carlos Castillo-Chavez, Baojun Song, Dynamical models of tuberculosis and their applications, Math. Biosci. Eng. 1 (2) (2004) 361.
- [76] Jack Carr, Applications of Centre Manifold Theory, vol. 35, Springer Science & Business Media, 2012.
- [77] H Rwezaura, ML Diagne, A Omame, AL de Espindola, JM Tchuenche, Mathematical modeling and optimal control of SARS-CoV-2 and tuberculosis co-infection: a case study of Indonesia, Model. Earth Syst. Environ. 8 (4) (2022) 5493–5520.
- [78] Expeditho Mtisi, Herieth Rwezaura, Jean Michel Tchuenche, A mathematical analysis of malaria and tuberculosis co-dynamics, Discrete Contin. Dyn. Syst. Ser. B 12 (4) (2009) 827–864.
- [79] N Ringa, ML Diagne, H Rwezaura, A Omame, SY Tchoumi, JM Tchuenche, HIV and COVID-19 co-infection: A mathematical model and optimal control, Inform. Med. Unlocked 31 (2022) 100978.
- [80] Bruno Buonomo, A simple analysis of vaccination strategies for rubella, Math. Biosci. Eng. 8 (3) (2011) 677-687.
- [81] Andrea Di Liddo, Optimal control and treatment of infectious diseases. The case of huge treatment costs, Math. 4 (2) (2016) 21.
- [82] Drew Posny, Jin Wang, Zindoga Mukandavire, Chairat Modnak, Analyzing transmission dynamics of cholera with public health interventions, Math. Biosci. 264 (2015) 38–53.
- [83] Hamadjam Abboubakar, Albert Kouchéré Guidzavaï, Joseph Yangla, Irépran Damakoa, Ruben Mouangue, Mathematical modeling and projections of a vector-borne disease with optimal control strategies: A case study of the Chikungunya in Chad, Chaos Solitons Fractals 150 (2021) 111197.
- [84] Lili Liu, Xi Wang, Ou Liu, Yazhi Li, Zhen Jin, Sanyi Tang, Xia Wang, Valuation and comparison of the actual and optimal control strategy in an emerging infectious disease: Implication from a COVID-19 transmission model, Infect. Dis. Model. (2024).
- [85] Erika Asano, Louis J Gross, Suzanne Lenhart, Leslie A Real, Optimal control of vaccine distribution in a rabies metapopulation model, Math. Biosci. Eng. 5 (2) (2008) 219–238.
- [86] Zenebe Shiferaw Kifle, Legesse Lemecha Obsu, Co-dynamics of COVID-19 and TB with COVID-19 vaccination and exogenous reinfection for TB: An optimal control application. Infect. Dis. Model. 8 (2) (2023) 574–602.
- [87] Kalyanasundaram Madhu, et al., Optimal vaccine for human papillomavirus and age-difference between partners, Math. Comput. Simulation 185 (2021)
- [88] Abboubakar Hamadjam, Kamgang Jean Claude, Optimal control of arboviral diseases, in: Proceedings of CARI, 2016, p. 445.
- [89] Hamadjam Abboubakar, Jean Claude Kamgang, Leontine Nkague Nkamba, Daniel Tieudjo, Bifurcation thresholds and optimal control in transmission dynamics of arboviral diseases, J. Math. Biol. 76 (2018) 379–427.
- [90] LS Pontryagin, VG Boltyanskii, RV Gamkrelidze, EF Mishchenko, The maximum principle, Math. Theory Optim. Process. New York: John Wiley Sons (1962).
- [91] Wendell H. Fleming, Raymond W. Rishel, Deterministic and Stochastic Optimal Control, Springer-Verlag, 1975.
- [92] L Pontryagin, V Boltyanskii, R Gamkrelidze, E Mishchenko, John Wiley & Sons; New York/London: 1963, Math. Theory Optim. Control. Process. 4 (1962).
- [93] Suzanne Lenhart, John T. Workman, Optimal Control Applied to Biological Models, 5-33, CRC Press, 2007, pp. 5-33.
- [94] JO Akanni, FO Akinpelu, S Olaniyi, AT Oladipo, AW Ogunsola, Modelling financial crime population dynamics: optimal control and cost-effectiveness analysis, Int. J. Dyn. Control 8 (2) (2020) 531–544.
- [95] Joshua Kiddy K Asamoah, Eric Okyere, Afeez Abidemi, Stephen E Moore, Gui-Quan Sun, Zhen Jin, Edward Acheampong, Joseph Frank Gordon, Optimal control and comprehensive cost-effectiveness analysis for COVID-19, Results Phys. (2022) 105177.
- [96] Eric Okyere, Samson Olaniyi, Ebenezer Bonyah, Analysis of zika virus dynamics with sexual transmission route using multiple optimal controls, Sci. Afr. 9 (2020) e00532.
- [97] Utami Dyah Purwati, Firman Riyudha, Hengki Tasman, et al., Optimal control of a discrete age-structured model for tuberculosis transmission, Heliyon 6 (1) (2020) e03030.
- [98] Habtamu Ayalew Engida, Modelling environmental-born melioidosis dynamics with recurrence: An application of optimal control, Results Control. Optim. (2024) 100476.